TECHNISCHE UNIVERSITÄT WIEN
Vienna | Austria

Master Thesis

Design of the inlet flow of a hydraulic reservoir to prevent structural damage

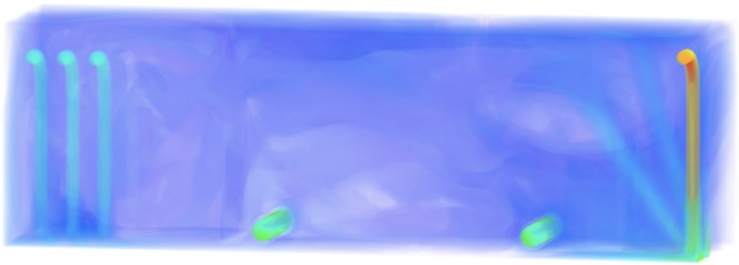

carried out for the purpose of obtaining the degree of Master of Science (MSc or Dipl.-Ing. or DI), submitted at TU Wien, Faculty of Mechanical and Industrial Engineering, by

Philip SCHWILLINSKY, BSc.

Mat.Nr.: 01325757

[redacted]

under the supervision of

Privatdoz. Francesco ZONTA, MSc. PhD.,

Institute of Fluid Mechanics and Heat Transfer, E322

Vienna, December 9, 2021

Author's e-mail:

philip.schwillinsky@tuwien.ac.at

Author's address:

Institute of Fluid Mechanics and Heat Transfer

Vienna University of Technology

Tower BA/E322, Getreidemarkt 9

1060 Vienna – Austria

Cover:

Volume rendering of the velocity field of a hydraulic reservoir

Abstract

Hydraulic power supplies are often chosen as an energy source in industry applications. Because of their reliability and high power density these units are very popular in high demanding tasks. One of these applications are injection moulding machines. High oil quality is the requirement to ensure a highly functional power unit. Therefore, the hydraulic reservoir must take care of maintaining the oil quality on a high level. One way to achieve this is to harmonise the flow filed.

This research work focuses on the impact of the flow state of different inlet configurations of a prismatic shaped hydraulic reservoir. The layout of the tank consists of a few inlets and two outlets. To obtain an in-depth view of the flow state inside the tank CFD simulations were carried out. The standard inlet pipe configuration is compared to a newly diffuser design to reveal changes of swirling within the hydraulic reservoir. The convergence behaviour was determined by an analysis of different meshes with varying resolution. The investigation of the diffuser was done separately to obtain a better view of flow characteristics of the diffuser itself.

For modelling turbulence flow the SST k-ω model was applied. All CFD simulations are carried out with *ANSYS Fluent V2020R2*. The post-CFD data is displayed within *ANSYS CFX* post CFD toolbox.

The outcome of this research work presents that changes of the inlet configuration may lead to less mechanical stress on the reservoir's structure. In particular an adaptation of the thickness of the plates to lower values appears reasonable. Additionally the newly diffuser design effects the swirling behaviour in a positive manner.

Zusammenfassung

Hydraulische Antriebsaggregate sind in vielen Bereichen der Industrie heutzutage nicht mehr wegzudenken. Gerade aufgrund ihrer Zuverlässligkeit und hohen Leistungsdichte qualifizieren sie sich für den Einsatz von anspruchsvollen Tätigkeiten, wie es beispielsweise der Fall von Spritzgießmaschinen ist. Um ein effizient arbeitendes Aggregat zu gewährleisten, muss eine hohe Güteklasse der Hydraulikfüssigkeit sichergestellt werden. Eine Möglichkeit um Einfluss auf die Qualität des Hydrauliköls zu nehmen ist, das Strömungsfeld zu beruhigen und Verunreinigungen zu vermeiden.

Die Auswirkungen von unterschiedlich gestalteten Zuläufen auf das Strömungsfeld eines Hydrauliktanks werden in dieser Forschungsarbeit genauer untersucht. Bei dem Hydraulikbehälter handelt es sich um einen quaderförmigen Tank mit vier Zuleitungen und zwei Abläufen. Es wurden CFD-Simulationen des Hydrauliktanks gemacht, um ein besseres Verständnis über das Strömungsfeld zu bekommen. In dieser Arbeit werden die Vor- und Nachteile von typischen in der Industrie eingesetzten Zuläufen mit einem neuartigen Diffuser-Layout verglichen. Der Fokus liegt auf der Entwicklung des Strömungsfeldes und den entstehenden Verwirbelungen. Um ein besseres Bild der Auswirkungen des Diffusers auf das Strömungsfeld zu haben, ist das Diffuser-Design isoliert betrachtet worden. Das Konvergenzverhalten ist mit unterschiedlich feinen Vernetzungen überprüft worden.

Um das Turbulenzverhalten im Tank beschreiben zu können wird vom SST k-ω Modell Gebrauch gemacht. Sowohl die CFD-Simulationen als auch die Auswertung und Darstellung der CFD Daten sind mittels *ANSYS Fluent V2020R2* und *ANSYS CFX* durchgeführt worden.

Die Ergebnisse dieser Arbeit zeigen auf, dass eine Adaptierung der Zuläufe die mechanische Belastung auf die Struktur des Hydrauliktanks reduzieren kann. Zusätzlich werden durch die lamellare Anordnung der Bleche des Diffusers die Verwirbelungen verringert.

Acknowledgments

Knowledge isn't power until it is applied.

Dale Carnegie

In reference to this quote I would like to thank Privatdoz. Francesco ZONTA, MSc. PhD. for inspiring me with his open minded and challenging advice and for always taking his time to answer all my questions during my work for this master's thesis.
It has been an honour to work on an ongoing technical issue under the supervision of Dipl.-Ing. Dr. Lukas MUTTENTHALER, BSc. He always has spared time to support my work, showed me his expertise in CFD analysis and had given me a better understanding of fluid dynamic processes of injection moulding machines.
Without their guidance and expertise in this subject this thesis would have not been feasible.
Special thanks to Univ.Prof. Dipl.-Ing. Dr.-Ing. Alfredo SOLDATI and the support of all your colleagues. It has been a privilege to write my thesis at the department of fluid dynamics and heat transfer in one of your working groups.

I am very grateful for the support of my friend Valentina, who taught me to embrace all challenges in life and never give up.
Special thanks to my study colleagues throughout my study period. You have shown me what it means to overcome difficulties, show endurance and truly enjoy success together. Thanks for sharing these memories with you Benedikt, Lukas, Sophie, Patricia, Philippe and Thaddäus.

I dedicate this work to my family which has always supported and encouraged me unconditionally on my educational path.
This one's for you.
P

Nomenclature

Physics Constants

$\boldsymbol{g}$	Gravitational constant $6.67430 \times 10^{-11}\,\mathrm{m}^3/(\mathrm{kg\,s}^2)$

Greek symbols & mathematical operators

α	Expansion coefficient
α^*	Coefficient of a low Reynolds number correction
α_B	Bunsen coefficient
α_{H_2O}	Water content
β	Given function to obtain dissipation of ω
$\boldsymbol{\tau}$	Second order Newtonian stress tensor
Γ_k	Effective diffusivity of turbulent kinetic energy
Γ_ω	Effective diffusivity of specific dissipation rate
λ	Thermal conductivity
μ	Dynamic viscosity
μ_{turb}	Turbulent viscosity
∇	Nabla operator
ν	Kinematic viscosity
ν_{turb}	Turbulent kinematic viscosity
ω	Specific dissipation rate
ρ	Friction index

Latin symbols

$\boldsymbol{F}$	Force
$\boldsymbol{f}$	Volumetric force density
$\boldsymbol{u}$	Velocity field
$\boldsymbol{x}$	Position
a_1	SST k-ω model constant
c_l	Concentration of a substance in a liquid medium
D_ω	Cross-diffusion term
e	Internal energy
G_b	Buoyancy term in k-equation
G_k	Production of turbulent kinetic energy
$G_{\omega b}$	Buoyancy term in ω-equation
G_ω	Production of specific dissipation rate
H	Henry's law constant
h	Enthalpy
k	Turbulent kinetic energy
L_{H_2O}	Life expectancy parameter as a function of water
L_P	Life expectancy parameter as a function of oil purity
p	Pressure
p_g	Partial pressure of a gas
Pr_t	Turbulent Prandtl number
S	Strain rate magnitude

s	Entropy
S_k	User-defined sources
S_ω	User-defined sources
t	Time
Y_k	Dissipation of turbulent kinetic energy
Y_ω	Dissipation of specific dissipation rate
z	Height

Acronyms

BSL	Baseline
CAD	Computer Aided Design
CBM	Condition Based Maintenance
CFD	Computational Fluid Dynamics
ERF	Explicit Relaxation Factors
FEA	Finite Element Analysis
ISO	International Organisation of Standardisation
ppm	Parts Per Million
$RANS$	Reynolds Averaged Navier-Stokes
RTD	Residence Time Distribution
SST	Shear Stress Transport
UDF	User-Defined Function

Contents

1

Introduction

If I have seen further than others, it is by standing upon the shoulders of giants.

Sir Isaac Newton

Hydraulic circuits are a widely used in industry and are known as reliable power units. Many applications demand a quite powerful energy source but also as little maintenance work as possible. Depending on the choice of the layout of a hydraulic tank the expenses of operation and maintenance may be tremendous due to poor decisions during the designing phase [1].

Often the never-ending story of achieving the ideal layout of engineering components appears to be an impossible challenge to solve. This is caused by the complexity of the multi physics problem of a real hydraulic container. The combination of different areas of technology, e.g. fluid dynamics, mechanical engineering, electronics and the use of sensors, makes the developing process even more difficult than it already appears [1, 2]. To master this issue of a reservoir's conception none of the above mentioned technologies should be neglected to obtain a powerful hydraulic power unit.

The main characteristic of a hydraulic tank is the possibility of storing a liquid medium. The efficiency of a hydraulic power unit on the other hand does not only depend on a simple storage space for the hydraulic medium. Many determining factors like the geometric shape, heat transfer, sloshing effects and easy access for maintenance work are decisive for a well functioning hydraulic circuit. Bad choices in design only reveal themselves while operating over time and are frequently caused by quite conservative

layouts and oversimplifications of the reservoir itself [3]. Therefore, the use of virtual engineering techniques has tremendously increased over the last decade. Computational fluid dynamic methods have not only been explicitly used in the aerospace industry but also research work of the behaviour of the fluid domain in various reservoir layouts has been conducted with CFD techniques [3–10].

Even if the complexity of real hydraulic tanks place high demands on computational methods like CFD or FEA, the benefits of using these techniques in the designing progress of a proper working hydraulic reservoir are huge. Not only the efficiency of the power unit increases but also to obtain a better knowledge of the ongoing physical processes.

1.1 Tasks & goals

The major challenge of this research work is based on a weight reduction of the whole injection moulding machine in general. One of the heavy parts of the machinery affects the hydraulic power unit, particularly the hydraulic reservoir. Since the original layout of the tank has been heavily reinforced due to structural problems, like leakage and cracks, the whole structure of the storage unit must become lighter. Therefore, the analysis of the present state of the hydraulic tank and a new proposal for the inlet configuration has been accurately studied in this thesis. The comparison of the given inlet designs should help to identify critical areas of the flow field and zones of high mechanical stresses.

The objective of this research work is to obtain a precise view on the inlet layout based on a lower stress state of the tank's structure and an enhanced flow field to lower undesirable swirling. This may enhance future development of hydraulic reservoirs in injection moulding machines. Always with the ulterior motive to push technological progress and effectiveness forward.

2

Functionality of hydraulic reservoirs

All our knowledge has its origins in our perceptions.

LEONADRO DA VINCI

Many companies which rely on hydraulic systems as a power unit often neglect the effectiveness of a proper functional hydraulic tank. As a rule hydraulic containers are designed of thin sheets of metal [3]. Depending on the properties of the oil reservoir they are made out of steel sheets, aluminium or cast iron. For larger constructed tanks welded steel plates are frequently used, while smaller ones are made of moulded or casted materials [11]. Two of the most used shapes in the industry for these tanks are cylindrical and prismatic ones. The choice of the design is important and ought to facilitate maintenance access and monitoring the condition of the oil [11, 12].

Beside its main function of storage space of a liquid, hydraulic reservoirs must fulfil other functions like the separation of gaseous, liquid and solid contamination, temperature management and easy access for maintenance [1, 11–14]. Therefore a proper design does not only help to identify and stabilise flow patterns which may lead to problems during operational time, but also to keep the oil quality on a high level. Poor oil quality leads to insufficient functionality of the hydraulic system which causes component damage, noise development, reduction of system stiffness, machine downtime, loss of lubrication, wear, costs and tremendous fluid degradation [1, 8, 12]. In many cases the interrelation of the above mentioned effects may lead to complications and issues of the whole machinery. The hydraulic container also represents the only easy access point in

the hydraulic system, where the mineral oil can be monitored and conditioned [8]. Regarding the mentioned arguments above the hydraulic pump and reservoir accordingly are called the *"heart"* of a hydraulic power unit. The same metaphor applies for the synthetic or mineral oil as the *"blood"* of one of these hydraulic systems. Thus, both elements should be taken into account as machine components and be properly monitored [13, 15]. The huge challenge in designing an efficient hydraulic reservoir does lie in taking multiple aspects like flow pattern, temperature control, separation effects, contamination processes and maintenance access into account. Not to focus merely on the primarily task of storage space but to identify the bigger picture of the purpose of a hydraulic tank. Only with a proper reservoir it is possible to achieve high hydraulic oil quality and thereby sustain almost ideal operating conditions.

2.1 Main function

Over the recent years manufacturers centre their attention during the development phase on a more powerful and efficient hydraulic power unit [16]. This pretty challenging engineering task often correlates with a hydraulic reservoir's primarily function of storage space for a fluid domain. This main function of storing liquid substances also includes oil level compensation as a cause of temperature variations, leakage of the hydraulic system and compressibility of the hydraulic medium [1, 8, 13, 14]. In most cases those storage containers are poorly designed. The most common shape of a hydraulic tank is a simple prismatic layout. There must be a rethinking of the very conservative way of designing a storage unit for fluid domains. This lack of knowledge leads to an increase of oil amount and improper functionality of the system caused by impurities within the hydraulic medium. The use of an optimised layout of a hydraulic reservoir helps reduce the tank's measurements, lower the costs for service work and especially diminish the fluid volume in use [3, 13, 16].
A properly designed hydraulic reservoir is more than just a regular storage unit and helps to maintain the properties of the hydraulic medium [1].

2.2 Temperature management

Nowadays storage containers of hydraulic fluids must fulfil another main function of temperature control besides the supply point of a fluid domain. During the dwelling time of the hydraulic liquid in the reservoir it allows the fluid to cool down and regain its properties. Due to the thermal expansion of the hydraulic liquid it is necessary to take the oil volume changes inside the container into account [1, 3]. To achieve a good heat dissipation the thermal properties of the used materials for the reservoir play an fundamental role. While the hydraulic fluid passes through the system the temperature of the working fluid increases and the heat must be emitted through the surface of the storing container. Often this is achieved by the simple phenomenon of natural convection. Typical working temperatures of hydraulic system lie within 40 °C to around 60 °C [1, 11].

Another way to take care of the temperature development is to cool the hydraulic fluid itself. Heat exchangers with particular closed systems have been showing some pretty good results. Free air-cooled systems are a very practical but also an expensive practical alternatives [11].

2.3 Contamination of hydraulic fluids

Modern hydraulic oils are used for several applications in the industry. Inevitably hydraulic fluids contaminate during the operating time of the machinery. Those contaminates can be of any kind of the three major states of aggregation: gaseous, liquid and solid.

To be precise a contaminant is described as any foreign material in a hydraulic fluid, which reduces the system's performance. The reason for this decrease of the fluid performance is due to deteriorating effects of the hydraulic fluid [17]. An overview of the different sources of contamination and their implications are shown in figure 2.1. The key element to lower the content of contaminants in a hydraulic reservoir is a properly working separation process of undesirable foreign matter [12, 16].

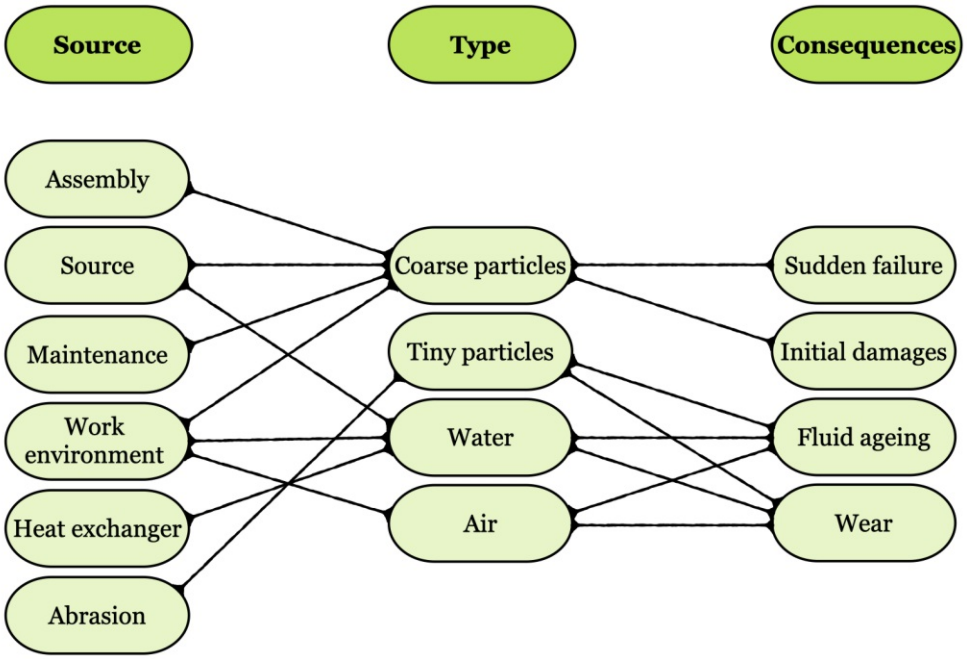

Figure 2.1 – Overview contamination sources

2.3.1 Gaseous contamination

Entrained air in a hydraulic power unit is the dominating part of gaseous contamination in hydraulic liquids. Usually air in hydraulic fluids can be found as solute and undissolved, e.g. air bubbles. According to Henry's law of solubility the amount of a dissolved gaseous substance in a liquid is proportional to its partial pressure in vapour phase [9, 18]. This relation can be written as [18, 19],

$$H = \frac{c_l}{p_g}, \tag{2.1}$$

where H represents Henry's law constant, c_l the concentration of a substance in a liquid medium and p_g describes the partial pressure of the gas. In literature Henry's law constant is frequently referred to as K. The concentration c_l can be expressed by the Bunsen coefficient α, which defines the solubility of air in a fluid medium [20, 21]. Typical values for the Bunsen coefficient α_B constitute around 9 % volume fraction of air in a standard mineral oil at atmospheric pressure. In general the solubility of air primarily depends on the oil type and pressure. Commonly the temperature, viscosity and additives have less contribution to the Bunsen coefficient α [6, 10, 20].

The cause for the detection of enclosed air lies in pretty noisy operating conditions of the components. Free air within a hydraulic circuit is undesired because of its impact on the power unit, but it is inevitable. In almost every case the design of the hydraulic reservoir plays a key role in the segregation and releasing process of the entrained air [1, 6, 16]. The change of physical and chemical properties of the oil has far reaching consequences ranging from declining cooling capacity, change of flow rate, increased oxidation of hydraulic fluid, pressure losses, noise pollution, machine downtime to raising costs for maintenance [3, 10, 13, 22].

This entrainment of air diminishes the efficiency factor of the hydraulic power unit itself and leads to an increase in energy consumption. Active measurements which help reduce the formation of air bubbles inside the hydraulic tank are a very promising approach. These measures contain easy to apply parts within the hydraulic reservoir like baffles, guide plates, diffusers and perforated baffles for fluid deaeration [1, 3, 12]. Another relatively new alternative is a so called hydrocyclone device. Its main function is based on a swirl flow inside a tapered tube which accelerates downstream [23].

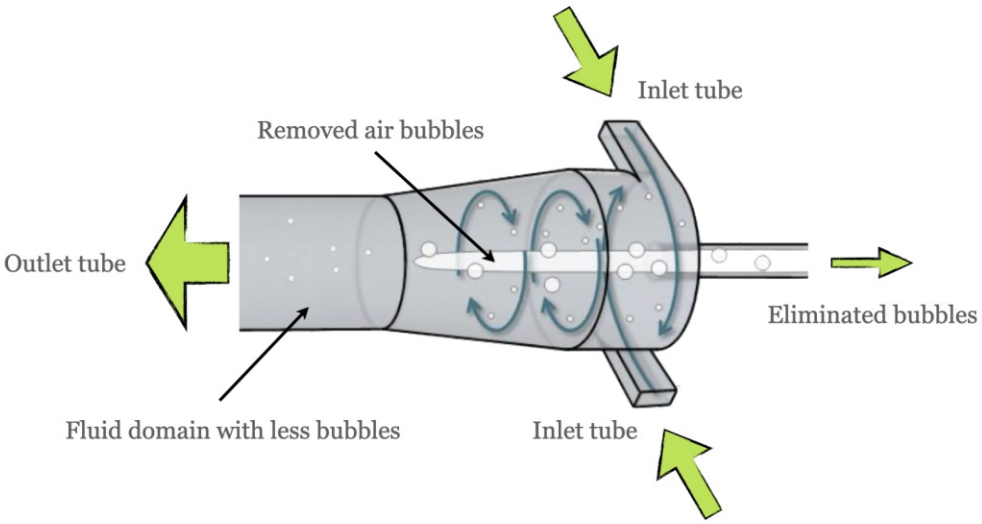

Figure 2.2 – Approach of a bubble removal component of a hydraulic unit

2.3.2 Liquid contamination

Almost always the liquid contamination of hydraulic fluids is related to the presence of water in such hydraulic power units. Frequently water enters the system during cleaning processes of the machinery, leakages in pipes and heat exchangers or through improper storage of hydraulic liquids. A fraction of the water content can be exchanged through ventilation filter in the reservoir. This may also lead to an increase of the water content as the moisture of the ambient atmosphere is absorbed [10]. There are three conditions how water can be found in oil:

- **Free water**
  water which quickly segregates to the bottom of the reservoir
- **Emulsified water**
  tiny globules of water dispersed in the hydraulic fluid; e.g. water in milk, fog in air, cosmetic products
- **Dissolved water**
  water molecules dissolved in the oil; like salt in water, humidity in air

Any non-binding water within the hydraulic fluid has a huge impact on the liquid's properties. Water decelerates the resistance of the hydraulic fluid against corrosion, diminishes lubrication, promotes hydrolysis and is accountable for rapid ageing of the lubricant [1, 10].
Gravely water contaminated systems as it occurs in the paper industry often must face a tremendously loss in viscosity and load capacity. These changes of properties in the hydraulic power unit due to higher water contents are the main source of damage and failure of components. Cavitation, a phenomenon known for its noise generation in the submarine industry also occurs in hydraulic power units with the presence of water. In areas of high pressure, commonly related to zones with high loading, vapour bubbles of water start to form and implode. In the process of the collapse of these droplets tiny micro-jets impinge the surrounding metal surfaces. In the end this leads to cavitation and pitting corrosion, which damage the effectiveness of the system [10, 24].
There is a recent study about the relation of the content of water in hydraulic oils and the durability of hydraulic components. Therefore, the water content α_{H_2O} is defined

as the volume fraction of water within the oil. To obtain a better view on the results, the life expectancy parameter L_{H_2O} and L_P is shown in two different ways in tables 2.1 and 2.2.

		Achieved ISO-Class									
		21/19/16	20/18/15	19/17/14	18/16/13	17/15/12	16/14/11	15/13/10	14/12/9	13/11/8	12/10/7
Original ISO-Class	24/22/19	2	3	4	5	7	9	>10	>10	>10	>10
	23/21/18	1.5	2	3	4	5	7	9	>10	>10	>10
	22/20/17	1.3	1.6	2	3	4	5	7	9	>10	>10
	21/19/16		1.3	1.6	2	3	4	5	7	9	>10
	20/18/15			1.3	1.6	2	3	4	5	7	>10
	19/17/14				1.3	1.6	2	3	4	6	8
	18/16/13					1.3	1.6	2	3	4	6
	17/15/12						1.3	1.6	2	3	4
	16/14/11							1.3	1.6	2	3
	15/13/10								1.4	1.8	2.5

Table 2.1 – Life extension factors for hydraulics and diesel engines [24]

As the results show the primarily durability will just be multiplied by the life expectancy parameter. [10, 24]. As table 2.2 shows, the lifetime will increase by the factor of 2 if the water content is lowered from 500 *ppm* to 125 *ppm* [12].

2.3.3 Solid contamination

In most cases solid particles are the number one reason for the majority of all failures in a hydraulic system. This solid contamination ought to be monitored very critical and with great accuracy. Almost 80 % of system failures are related to the consequences of solid particles in hydraulics [13]. Therefore, the life time of hydraulic components can be hugely affected by the presence of particles in the system [12]. The damage of hydraulic components created by the impact of solid particles within the system varies between 50 % to 85 %. Related to the overall system failure of around 80 % the majority of the cases are due to particles within the system [12, 24, 25]. This often appears as an impossible task to manage because even with particular filtration systems not all particles can be removed of the hydraulic unit. Again, the design of the reservoir plays

		Life Extension Factor L_{H_2O}								
		2	**3**	**4**	**5**	**6**	**7**	**8**	**9**	**10**
Moisture Level, *ppm*	**50 000**	12 500	6 500	4 500	3 125	2 500	2 000	1 500	1 000	782
	25 000	6 250	3 250	2 250	1 563	1 250	1 000	750	500	391
	10 000	2 500	1 300	900	625	500	400	300	200	156
	5 000	1 250	650	450	313	250	200	150	100	78
	2 500	625	325	225	156	125	100	75	50	39
	1 000	250	130	90	63	50	40	30	20	16
	500	125	65	45	31	25	20	15	10	8
	260	63	33	23	16	13	10	8	5	4
	100	25	13	9	6	5	4	3	2	2

Table 2.2 – Life extension expectancy relying on the use of mineral-based fluids. (1 % water = 10 000 *ppm*) [24]

a tremendous role to obtain the power over those solid particles. With a good layout of the tank there is potential to control the accumulation process of solid matter at the bottom plate [1]. In literature this state of particles scattered over a defined surface is described by a so called density function.

The influence of contamination does also depend on the shape, size, material and origin of the particles. Even if those particles possess specific wear and tear. In many cases the knowledge of the source of particle contamination aids to keep the hydraulic power unit as free as possible of foreign matter. The origin can be divided into several areas [10]:

- Manufacturing process
- Assembly
- Bringing into service
- Initial contamination of hydraulic fluids
- Maintenance

2.4 Condition Monitoring

To gather an in-depth view about the current state of many oil parameters condition monitoring is becoming more and more present in the industry. Observing the quality and oil properties, like water content, temperature, particle amount, oil viscosity, oil ageing progress and pressure helps to identify the ideal intervals for maintenance and service work. Often this process of monitoring properties of a hydraulic system has a huge contribution of improving the life expectancy of the machinery and lower maintenance expenses [10, 12, 15–17]. There are basically three approaches to observe oil or lubricant properties in the industry:

- **No monitoring**
  only if some issues appear;
- **Manually checks of the oil**
  samples are taken from the hydraulic unit and are analysed in the laboratory;
- **Automatic oil control systems**
  implemented filtration systems to keep oil free of contaminants;

Since the industry has become increasingly digitised over the last decade, manufacturing companies in specific industrial sectors have taken advantage of the opportunity and have developed their own CBM online system for their injection moulding machines [10, 15, 26]. To help save expenses and increase the availability of injection moulding machines those manufacturers do not want to rely on the experience of their staff when it comes to maintenance. The cause for the implementation of such monitoring systems is that often machine parts are replaced way earlier than necessary [26]. To help save expenses and increase the availability of injection moulding machines the company does not want to rely only on the experience of their maintenance staff. To collect the data of the hydraulic fluid special sensors are installed in the hydraulic circuit. With the obtained data critical conditions should be easier identified and sudden failure or damages can be prevented [15].

2.5 Maintenance & oil analysis

One of the most neglected aspects during the development of a hydraulic tank is a proper design for maintenance work. This leads to the consequence that the layout of the reservoir should facilitate maintenance operation as an easy access to the interior. As a fact the hydraulic container is the only location of the power unit where the hydraulic fluid can be conditioned and observed [1, 8].

Condition based monitoring plays a pioneering task in the manufacturing industry. But there are some challenges to overcome. Firstly, the major task is to accumulate precise real time data of the current condition of the hydraulic fluid to be able to efficiently respond to the situation. This provides a better knowledge about the present state of wear and tear of products. The other challenge is to coordinate maintenance intervals based on the collected data of the fluid. The analysed information about the current condition often leads to extended span of time between maintenance operation which implies an increase of the manufacturing plant availability [13, 27].

Besides monitoring of the fluid's properties, CBM often consists of an analysis of samples taken from the hydraulic power unit. Those laboratory examinations of the used fluids reveal an in-depth view about the water content, solid particles like wear debris, state of lubrication and are of major concern for manufacturing companies. The major quantities affecting the durability of the hydraulic medium are shown in figure 2.3. According to literature these laboratory investigations have been referred to a potential save of approximately 275 000 $ for industrial manufacturing plants because of avoided servicing measures and production uptime [17, 28].

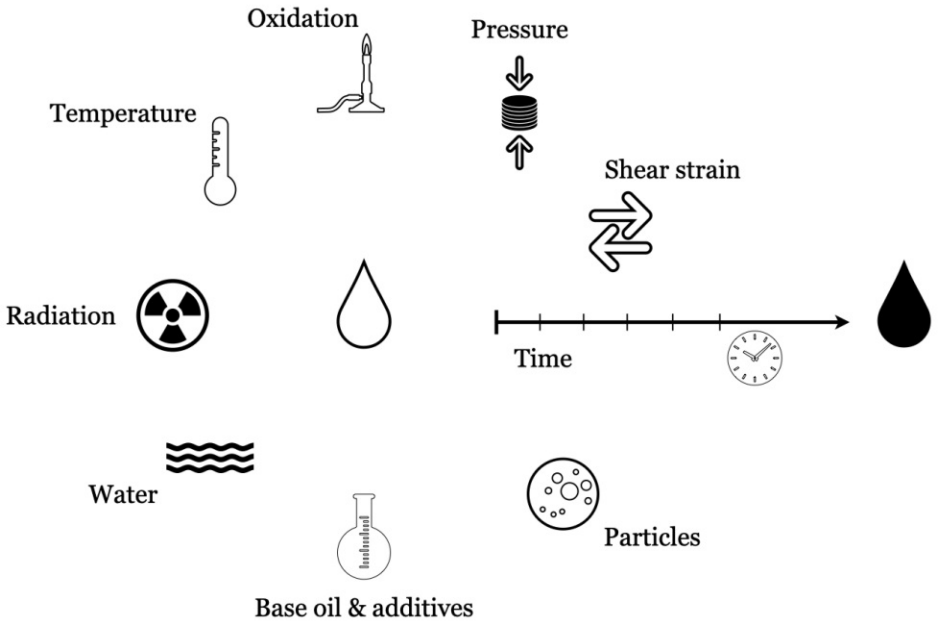

Figure 2.3 – Quantities which have an impact on the oil quality and cleanliness [10, 15]

2.6 Other engineering challenges

If the machinery is in motion, this will pose another sophisticated challenge on the design of a hydraulic reservoir. It is called sloshing. This phenomenon is founded on the interaction of a liquid domain and a solid structure. Often sloshing results from an improper layout of the tank. Baffles and other guided plates reduce the impact of large scale sloshing which may lead to damages caused by interaction of non-linear waves [4, 29, 30].

3

Virtual engineering

Measure what is measurable, and make measurable what is not so.

Galileo Galilei

The use of simulation methods or in general virtual engineering techniques is becoming more popular in the developing process of products over the last decade. Driven by the tremendous success of major industries like the automotive and aerospace branches, virtual engineering is getting established in other technical areas like hydraulic and pneumatic industry as well [1, 3]. These simulation techniques might be helpful in the designing process of complex products due to their difficult operating conditions. Even enterprises rely on simulation methods as a part of their innovation progress [1, 4, 5, 9]. With these possibilities of engineering the creation of often new and complex technology can be simplified before it's actual realisation [31].

Finite elements or computational fluid dynamics simulation plays a vital role in many engineering companies. This intersection of the use of CAD, CFD and FEA methods in designing and conception of new products has huge applications in the automotive, aerospace and mechanical industry in general. This way of analysing various designs of models before even producing a single prototype helps saving unnecessary production time, costs and eliminates test phases of preproduction models [4, 7, 32–34].

Those virtual engineering tools are driving a simulation based product development forward. Usually the stress state and boundary conditions in reality are often pretty

complicated, e.g. phenomenon of sloshing or the interaction of the fluid with the structure like baffles. Therefore the use of virtual engineering helps to reduce the complexity and makes the calculation process easier. In many cases the complexity of the reality presents challenges for the means of virtual engineering. Therefore great demands are placed on simulation techniques to achieve a high effectiveness in numerical tools for several applications [1, 4, 32]. One of these applications are hydraulic reservoirs, which will be further discussed in this work.

One of the major power units used by the industry are hydraulic systems. For many enterprises the key to their economic success lies in a high efficient and reliable power source. In order to obtain a highly functional hydraulic reservoir, many parameters like for example the material, surface coatings and the geometric shape of the tank, must be taken into account. Unfortunately many of the hydraulic tank designs are engineered in a very conservative way which are frequently justified with older generation models [1, 3, 9]. Despite that it happens that hydraulic systems are not considered as multidisciplinary which can lead to tremendous failures of the whole system at all. Nowadays hydraulics and pneumatics are getting more complex than in recent years. This progress of technology leads to the challenge to take multiple areas of engineering, e.g. electronics, sensorics, mechanics and informatics, during the conception of hydraulic systems into account [1].

In almost every case of developing a hydraulic reservoir space management and design complexity pose a huge challenge on the engineers. Therefore it is inevitable to not oversimplify the reservoir's design during the use of virtual engineering tools in order to achieve a tank with high efficiency [2, 3]. One of tools driving the development of complicated problems forward is CFD analysis. There are several applications where CFD simulation may be very useful to solve complex engineering problems [6, 8, 11, 12, 16, 27, 35]. Computational fluid dynamics methods help to easier identify flow pattern inside a hydraulic tank which indeed largely depend on the inflow configuration. The inlet characteristics have as a consequence a great impact on the stresses on the internal structure of the reservoir [2, 32].

Additionally almost every time non-linear effects occur in hydraulic systems due to the change of a laminar flow state to a turbulent one or the phenomenon of cavitation and aeration at low pressures. Virtual engineering methods like CFD simulation are not

only a promising approach in designing new products but also help to identify critical areas of already existing models. These zones of can then be adapted and improved for a better tank performance and redesigned layout [1, 2].

With all these aspects put together CFD analysis appears to be a highly powerful tool to enable future efficiency improvement and optimisation of hydraulic reservoirs for industrial applications [1, 3, 13].

4

Methodology

Intelligence is the ability to adapt to change.

STEPHAN HAWKING

In reality flow patterns within a hydraulic reservoir are a very complex and three dimensional flow state. Sometimes physical phenomena like cavitation, multiphase flow and free surface flow are neglected to simplify reality. In this research work only the impacts of the intricate fluid flow state on the solid structure are investigated.

4.1 Conservation of mass

Based on published research [2, 3, 13, 32, 35, 36] almost every viscous fluid dynamic simulation is predicated on the basic equation of mass conservation described in an inertial reference frame, respectively the continuity equation [37, 38],

$$\frac{\partial \rho}{\partial t} + \nabla \cdot (\rho \mathbf{u}) = 0. \tag{4.1}$$

As is common practice hydraulic fluids can be assumed as incompressible with a constant density $\rho = const.$. Thus, the time derivative term $\frac{\partial \rho}{\partial t}$, which represent the change of mass, can be neglected. It remains a simpler form of the mass conservation formulation,

$$\nabla \cdot (\rho \mathbf{u}) = 0. \tag{4.2}$$

4.2 Conservation of momentum

Besides the conservation of mass the fluid domain needs also to be characterised by the acting momentum, which is described by the following equation of momentum conservation [37, 38],

$$\rho \frac{\mathrm{D}\mathbf{u}}{\mathrm{D}t} = -\nabla p + \nabla \cdot \boldsymbol{\tau} + \rho\,\mathbf{g} + \mathbf{F} \tag{4.3}$$

with the material derivative

$$\frac{\mathrm{D}\mathbf{u}}{\mathrm{D}t} = \frac{\partial \mathbf{u}}{\partial t} + \mathbf{u} \cdot \nabla \mathbf{u} \tag{4.4}$$

which characterises the acceleration or in general the rate of change of a physical property of a substantial fluid volume element. The term $\boldsymbol{\tau}$ is representing a second order Newtonian stress tensor. The acceleration acting on the body by the gravity for instance is illustrated by $\mathbf{g}$. The last expression should identify external forces acting on the fluid continuum and can also be written as,

$$\rho\,\mathbf{f} = \mathbf{F}, \tag{4.5}$$

with $\mathbf{f}$ as the volumetric force density. These formulations of the conservation of mass (equation 4.1) and momentum (equation 4.3) are also referred to as the Navier-Stokes equations [37].

4.3 Reynolds averaged Navier-Stokes equations

The used formulations of physical laws for this turbulent flow are the so-called Reynolds-averaged Navier-Stokes-equations, short $RANS-$equations. Consistently particular details of a turbulent and fluctuating flow are not of interest in the calculating process. Therefore Reynolds has introduced a decomposition of a physical quantity, like pressure p or velocity u, into its temporal mean value and fluctuating component [10, 37, 38],

$$\mathbf{u}(\mathbf{x},\, t) = \overline{\mathbf{u}}(\mathbf{x}) + \mathbf{u}'(\mathbf{x},\, t). \tag{4.6}$$

with the correlation,

$$\overline{f(t)} = \lim_{T\to\infty} \frac{1}{2T} \int_{-T}^{T} f(t)\,\mathrm{d}t \qquad \text{and} \qquad \overline{f'(t)} = 0. \tag{4.7}$$

Quantities with a dash represent the fluctuating components with their corresponding mean value. This formulation is then applied in the conservation of mass and momentum equations and leads to the so called *Reynold's equations*,

$$\overline{\mathbf{u}} \cdot \nabla \overline{\mathbf{u}} = -\frac{1}{\rho}\, \overline{p} + \nu \nabla^2 \overline{\mathbf{u}} - \overline{\mathbf{u}' \cdot \nabla \mathbf{u}'} \tag{4.8a}$$

$$\nabla \cdot \overline{\mathbf{u}} = 0 \tag{4.8b}$$

where ρ corresponds to the density of a given substance and ν represents the kinematic viscosity, defined in equation (5.2) Assuming that the temporal average value of the fluctuating component is equal to zero, according to (4.7), leads to the substitution of the physical quantities by their mean values. There is one exception which correlates to an additional term $\overline{\mathbf{u}' \cdot \nabla \mathbf{u}'}$, representing turbulent stresses, in the momentum equation. This term represents the temporal averaging of the product of two fluctuating quantities, which have a mean value equal to zero. Analogous to the averaged Navier-Stokes equation (4.8a) one can derive this above mentioned additional term and the viscous term $\nabla^2 \overline{\mathbf{u}}$ by the divergence on a stress tensor [37],

$$\mu \nabla^2 \overline{\mathbf{u}} - \rho \overline{\mathbf{u}' \cdot \nabla \mathbf{u}'} = \nabla \cdot \left\{ \underbrace{\mu \left[\nabla \overline{\mathbf{u}} + (\nabla \overline{\mathbf{u}})^T \right]}_{viscous\ part\ of\ tensor} - \underbrace{\rho \overline{\mathbf{u}'\mathbf{u}'}}_{turbulent\ part\ of\ tensor} \right\} \tag{4.9}$$

This latter expression is referred to as the turbulent stress tensor in the literature [37],

$$-\rho \overline{\mathbf{u}'\mathbf{u}'} = -\rho \begin{pmatrix} \overline{u'u'} & \overline{u'v'} & \overline{u'w'} \\ \overline{v'u'} & \overline{v'v'} & \overline{v'w'} \\ \overline{w'u'} & \overline{w'v'} & \overline{w'w'} \end{pmatrix}. \tag{4.10}$$

This tensor consists of turbulent tangential stresses, like $(-\rho\overline{u'u'})$, and perpendicular stresses, e.g. $(-\rho\overline{u'v'})$, are frequently referred to as Reynold's stresses [10, 37].

4.4 Turbulence - Shear Stress Transport Model

There are many turbulence models used by the industry to obtain a better understanding of the ongoing fluid dynamic processes in reality [2, 4, 13, 35]. The applied model in this research work to simulate turbulence flow within the reservoir is the Shear-Stress Transport k-ω model, abbreviated SST k-ω model. The SST k-ω approach is based on the empirical standard and baseline k-ω model, but in general the SST, BSL and standard model have a similar formulation with some adaptions depending on the application. The few changes which are made between the standard and SST models are related to the flow regions and the turbulent viscosity formulation [38, 39].
This model combines the robustness and good performance of the Wilcox k-ω approach for near wall areas. Simultaneously it benefits of the models free stream independence in the outer boundary layers. As the Wilcox model is highly sensitive to free stream which has an impact on the values of k and ω [40]. For the flow regions an alteration of the applied approach is made. While the inner part of the boundary layer will be calculated with the k-ω model, the outer region of the boundary layer and free shear flows are computed with the k-ε model. The transition of the two approaches takes place successively. The other significant difference accounts for the transport effects of turbulent shear stress. This adjustment of the eddy viscosity leads to major improvements in the prediction of adverse pressure gradient flows, airfoils and transonic shock waves [38]. The underlying principle for this forecast is the transport of turbulent shear stress. Thus, this model is often applied in aerodynamic simulations and applications [39].

4.4.1 Turbulent kinetic energy

The turbulent kinetic energy formulation of the SST k-ω model has its origin in the transport equations of the standard k-ω approach. In addition it also implies the above mentioned effects on the turbulent viscosity μ_{turb} in order to not obtain an over prediction of the eddy viscosity [38]. The transport equation for the turbulent kinetic energy k has all enhancements of the BSL k-ω model and k is obtained from the following formulation [38],

$$\frac{\partial}{\partial t}(\rho k) + \frac{\partial}{\partial x_i}(\rho k u_i) = \frac{\partial}{\partial x_j}\left(\Gamma_k \frac{\partial k}{\partial x_j}\right) + G_k - Y_k + S_k + G_b. \tag{4.11}$$

The effective diffusivity of the turbulent kinetic energy Γ_k is determined by the subsequent relation,

$$\Gamma_k = \mu + \frac{\mu_{turb}}{\mathrm{Pr}_t}, \tag{4.12}$$

in which Pr_k represents the turbulent *Prandtl number*. The advantage of the shear stress transport k-ω model lies in the formulation of the eddy viscosity. Besides all the improvements of the BSL model, the transport of turbulent shear stress is taken into account with this given correlation,

$$\mu_{turb} = \frac{\rho k}{\omega} \cdot \frac{1}{\max[\frac{1}{\alpha^*}, \frac{SF_2}{a_1 \omega}]}, \tag{4.13}$$

in which α^* stands for a coefficient of a low Reynolds number correction, S representing the strain rate magnitude and a_1 is one of the SST model constants. The other physical quantities are thoroughly described in the *ANSYS Theory Guide* [38].
According to equation (4.11) the term G_k accounts for the production of turbulent energy and is defined in a similar manner as (4.9) [38],

$$G_k = -\rho \overline{u_i' u_j'} \frac{\partial u_j}{\partial x_i} = -\rho \, \nabla \cdot \overline{\mathbf{u}'\mathbf{u}'}. \tag{4.14}$$

The expression Y_k identifies the dissipation of turbulent kinetic energy and is quite similar to the form of the original k-ω model. The only differences lies in the definition of the describing function of f_{β^*} [38],

$$Y_k = \rho\beta^* f_{\beta^*} k\omega \qquad \text{with} \qquad f_{\beta^*} = 1. \tag{4.15}$$

The detailed description for β^* is found in the *ANSYS Theory Guide* [38]. The other missing terms S_k and G_b of equation (4.11) represent on the one hand other energy source terms than the above described ones, often user-defined expressions. Otherwise G_b identifies the change of turbulent kinetic energy due to effects of buoyancy caused the presence of a non zero gravity field and temperature gradient.

4.4.2 Specific dissipation rate

Also the specific dissipation rate ω is obtained from the transport equation of the standard k-ω model but does have the improvements of the BSL model and is described as follows,

$$\frac{\partial}{\partial t}(\rho\omega) + \frac{\partial}{\partial x_i}(\rho\omega u_i) = \frac{\partial}{\partial x_j}\left(\Gamma_\omega \frac{\partial \omega}{\partial x_j}\right) + G_\omega - Y_\omega + D_\omega + S_\omega + G_{\omega b}. \tag{4.16}$$

Again, the effective diffusivity of the specific dissipation rate Γ_ω is obtained by the consecutively correlation,

$$\Gamma_\omega = \mu + \frac{\mu_{turb}}{Pr_t}. \tag{4.17}$$

According to this relation (4.19) the variable Pr_t relates to the turbulent *Prandtl number* and the turbulent viscosity μ_{turb} is computed as in equation (4.13). As well the adaptation of μ_{turb} associates in a proper transport behaviour of turbulent shear stress. Further explanations of definitions of variables are thoroughly documented in the *ANSYS Theory Guide* [38].

The term G_ω of the equation (4.16) is obtained by the following correlation of the production of turbulent kinetic energy G_k and scalar coefficient [38],

$$G_\omega = \frac{\alpha\alpha^*}{\nu_{turb}} G_k. \tag{4.18}$$

This formulation includes one of the important refinements of the BSL and SST k-ω model compared to the standard one. For the enhanced models α^* is computed via a given function instead of a constant value like it is the case of the standard k-ω approach. The precise details of the definitions of these parameters are registered in the *ANSYS Theory Guide* [38].
In comparison to the definition of the dissipation of turbulent kinetic energy Y_k the term Y_ω is formulated in a similar way [38],

$$Y_\omega = \rho\beta f_\beta \omega^2 \qquad \text{with} \qquad f_\beta = 1. \tag{4.19}$$

Y_ω illustrates the dissipation of ω itself. There is one additional term in equation (4.16) compared to the formulation of (4.11) which refers to cross diffusion expression D_ω. The origin of D_ω leads back to the combination of the k-ε and k-ω model on which the BSL approach is based on. Further details of the definitions are explained in [38].
The last missing expressions in equation (4.16) account for additional source terms S_ω and effects on buoyancy $G_{\omega b}$ in a similar manner to G_b from chapter 4.4.1.

5

Hydraulic reservoir analysis

I think you should always bear in mind that entropy is not on your side.

ELON MUSK

To simulate turbulent flow within a solid structure there are several softwares available on the market, which have the performance to fulfil such demanding simulations of complex problems. The chosen software package for this research work is *ANSYS Fluent 2020 R2*.

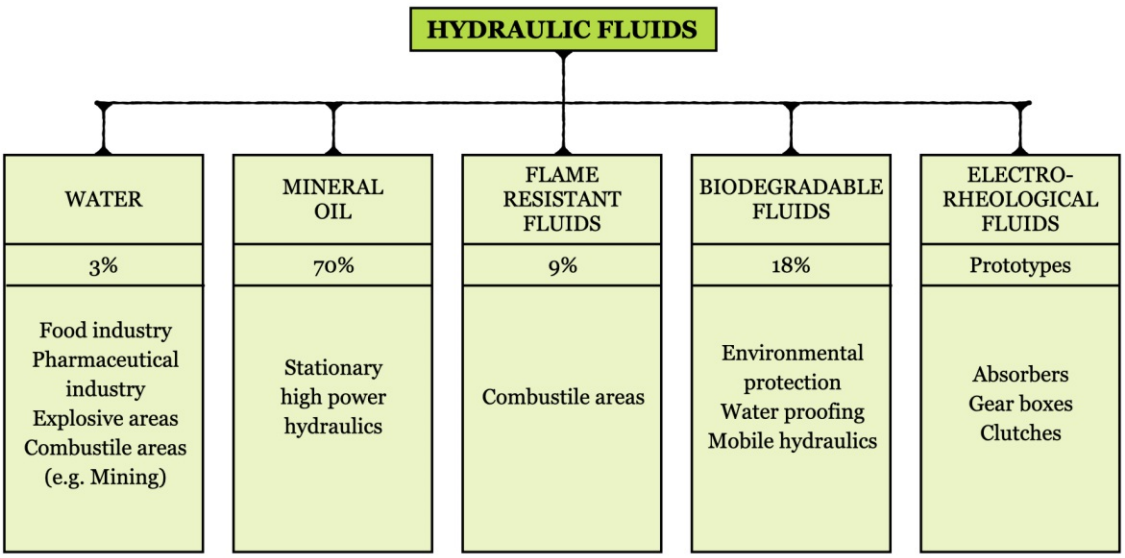

Figure 5.1 – Classification and use of hydraulic fluids [21]

5.1 Modern mineral & synthetic hydraulic oils

Hydraulic fluids are one of the major components of a hydraulic power unit. Since the middle of the 20th century a hydraulic medium based on mineral oil has been on the rise in many applications in the industry. Depending on the classification of these fluids, as shown in figure 5.1, they must fulfil certain requirements in a hydraulic power unit [10, 21, 41]:

- **Transfer of energy and pressure**
- **Good heat transfer capability**
- **Fire resistance**
- **Transport of solid impurities to the filtration system**
- **Environmental compatibility**
- **Non-toxicity**
- **Great lubrication**
- **Ideal viscosity**

Most of the hydraulic fluids consists of a base oil and additive compounds which enable a variety of the above mentioned properties. With those additive compounds chemical and physical properties can be selectively manipulated to achieve the high demands of a high-grade mineral or synthetic hydraulic medium [10]. Beside the classification according to the application areas hydraulic fluids are often classified by their ISO-viscosity grade. The viscosity is the fundamental part of the identification of hydraulic liquids and is characterised by the relation [21, 37],

$$\tau = \mu \frac{\partial u}{\partial n}. \tag{5.1}$$

The correlation (5.1) describes the acting shear force τ by the relative motion between two close-by layers of liquids in the perpendicular direction n of the wall. Thus, the velocity u must increase with further distance of the barrier. The dynamic viscosity η is proportional to the velocity gradient. Fluids which behave according to equation (5.1)

are referred to as Newtonian fluids [21, 37]. The kinematic viscosity ν is then defined over the density ρ of the liquid medium and the dynamic viscosity η [37],

$$\nu = \frac{\mu}{\rho}. \tag{5.2}$$

5.1.1 Properties of Lukoil Geyser ST 46

The simulation is carried out with a standard hydraulic oil as fluid medium. Precisely, it is an Lukoil Geyser ST 46, similar to an ISO VG 46, mineral oil provided by the oil company Lukoil. The oil features great ageing properties, improved tribological behaviour and has minor tendency to foaming. Typical applications for this mineral oil are heavily loaded hydraulic power units. It is used by companies like BOSCH REXROTH, PALFINGER and THYSSENKRUPP for their machineries [42]. The properties are shown in table 5.1. The data sheets and further details are given in the Appendix A.1. Both simulations of the hydraulic reservoir and the parameter study of the different diffuser designs are carried out with the exact same hydraulic oil.

		Lukeoil Geyser ST 46	
Physical quantities	Viscosity	46	$\frac{mm^2}{s}$
	Viscosity classification	ISO VG 46	-
	Molar mass	900	$\frac{kg}{kmol}$
	Density	878	$\frac{kg}{m^3}$
	Specific heat capacity	1950	$\frac{J}{kg \cdot K}$
	Thermal conductivity	0.131	$\frac{W}{m\,K}$

Table 5.1 – Properties of hydraulic fluid - Lukeoil Geyser ST 46 [42–46]

5.2 Shape & design

The layout of the hydraulic tank which ought to be analysed was designed within the CAD software *ANSYS SpaceClaim 2020 R2*. This reservoir is based on a simple prismatic shape as shown in figure 5.2, with a few improvements to the outer structure.

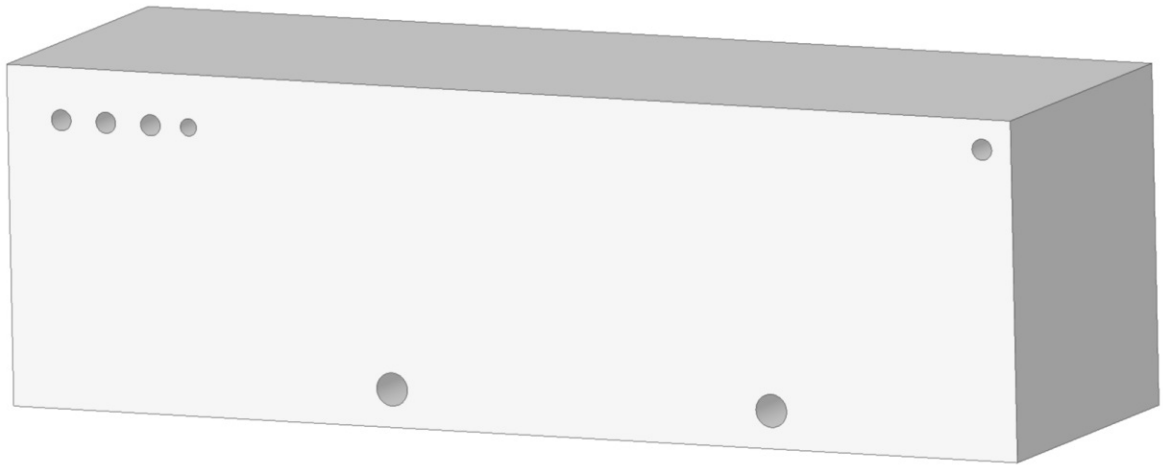

Figure 5.2 – Shape of the hydraulic reservoir

The capacity of the tank amounts to several hundred litres of hydraulic fluid to provide high volume flow rate during the injection process. The inside consists of an arrangement of several baffles at particular locations. The main purpose of these baffles is to deflect the flow of the inlet pipes. Those allow a three-dimensional deceleration of the liquid medium. It assists fluid deaeration, solid particles sedimentation and cooling of the fluid domain.

The layout of the baffles separates the straight linking of the hydraulic oil from the inlets to the outlets. These baffles do only have half of the thickness of the outer structure plates. Other unnecessary and inactive supply pipes or gaps in the steel plates were removed, respectively neglected. This simplification assists to reduce the computational effort of the simulation. As common practice in industry the supply and suction pipes of were cut at an angle of 45 ° [8]. There is one additional supply pipe added to the model in case of need of another feeding pipe of the hydraulic system. Other noticeable features of the hydraulic reservoir are related to the exterior structure.

5.3 Mesh

The mesh for the computational fluid dynamic simulation was created in *ANSYS Fluent 2020 R2*. More precisely, both the surface mesh and the volume mesh of the hydraulic reservoir itself were automatically computed in *ANSYS Fluent Mosaic Meshing*. In total three grids with a different number of elements for each of the models were created, as shown in table 5.2. Ranging from a lower quantity of elements to a higher number to

		Number of elements
Mesh	coarse	609 463
	standard	1 299 218
	fine	2 109 642

Table 5.2 – Overview of diverging grid elements

analyse the convergence behaviour. Additionally a few settings were adjusted to obtain a mesh with proper quality. The pattern of the mesh itself is better known as a mosaic meshing, illustrated in figure 5.3. The grid for the layout with straight supply tubes was built up of different size elements for the surface and the volume mesh. It consists of flow elements with a basic poly-hedral and poly-hexacore structure, added buffer and inflation layers. The latter ones are close to wall regions and do have an impact on the velocity gradients. As the maximum values occur in perpendicular direction to the solid structure [1]. Inflation layers were applied in each of the models with an expansion factor of 1.2 independent of the number of flow elements. The buffer layers consist of polyhedrons and were used for the transition to the poly-hexacore mesh, according to figure 5.3.

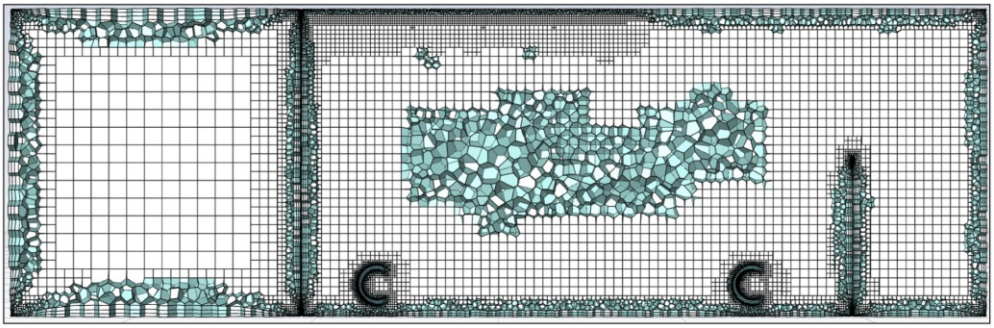

Figure 5.3 – Cut through mesh - cell layers overview

5.4 General setup of the simulation

The investigation of the predominating flow state of the hydraulic reservoir are realised by a three dimensional CFD analysis. The hydraulic tank is treated as completely filled. To help stabilise the solution a combination of a steady state and transient simulation is carried out.

5.4.1 Selected Models

The applied models strongly depend on the application to describe. Since the simulation of this hydraulic reservoir is a three dimensional one the choice of the right model is crucial for the CFD results. To obtain realistic simulation results of the ongoing physical processes inside a hydraulic reservoir the Shear Stress Transport k-ω model was used. The advantage of this model lies in the transition of free shear flow regions and wall regions. Depending on the regions the model describes the phenomena with two different approaches. There were no further adjustments of the model's default parameters values, respectively constants [47].

5.4.2 Boundary Conditions

The several types of boundary conditions of this physical problem are based on the restrictions of reality. It is assumed that there is a constant temperature of 40 °C and no temperature changes within the hydraulic reservoir during its operating conditions. The inlets are given as velocity inlets with no specific UDF. Besides the predetermined value of the inlet velocity also a turbulent intensity of 5 % and the hydraulic diameter of the inlet pipe is considered as a given value. The are changes in magnitude of velocity depending on the inlet port. All types of used boundary conditions are mentioned in table 5.3. The boundary conditions of the outlet ports do only depend on the pressure specifications. Therefore they are considered as pressure outlets with $0\,Pa$ gauge pressure. Other necessary boundary conditions are the stationary no-slip wall conditions for the outer structure and baffles of the hydraulic tank.

		Type
Bound. cond.	Inlet	velocity-inlet
	Outlet	pressure-outlet
	Wall	stationary/no-slip

Table 5.3 – Boundary conditions of the CFD analysis of the hydraulic reservoir

5.4.3 Methods & Controls

The basic setup for the analysis of the hydraulic tank is a combination of a pressure-based steady and transient simulation. The influence of gravity g is turned on. For the steady simulation part the warped-face gradient correction and the pseudo transient option is used. Also the discretization schemes are all set to second order for momentum, pressure, turbulent kinetic energy and specific dissipation rate with the objective to stabilise the CFD simulation.

After some adaptions to the explicit relaxation factors all values are set to their default ones as it provides the most realistic data about the reservoir. The specific values of the explicit relaxation factor are given in table 5.4.

		Values
Explicit Relaxation Factors	Momentum	0.5
	Pressure	0.5
	Density	0.25
	Body Forces	1
	Turbulent kinetic energy	0.75
	Specific dissipation rate	0.75
	Turbulent viscosity	1
	Energy	0.75

Table 5.4 – Explicit relaxation factors of hydraulic reservoir's CFD analysis

5.5 CFD - Analysis

For the convergence behaviour an analysis of different grid resolutions has been made. To obtain significant results not only the curve progression of the residuals are taken into account but also additional physical quantities are monitored. In general the convergence criteria is based on a practical approach of the industry. Therefore the conditions for the hydraulic tank are shown in table 5.5. These conditions must be fulfilled to obtain proper CFD results. The specific details about this investigation of varying mesh sizes are given in the Appendix A.2.

		Convergence criteria
Residuals	Continuity	$< 10^{-3}$
	x-velocity	$< 10^{-3}$
	y-velocity	$< 10^{-3}$
	k	$< 10^{-3}$
	ω	$< 10^{-3}$
	pressure at outlet	$< 10^{-3}$
	velocity at outlet	$< 10^{-3}$

Table 5.5 – Convergence criteria for the CFD analysis of the hydraulic reservoir

5.5.1 Results

There are several ways to evaluate the obtained CFD-analysis data. The most common and obvious one is to display the flow fields and the pressure distribution of the investigated problem. In this research work the examination of the velocity and pressure field acts as an indicator for any changes in the resolution of the grid itself. As illustrated in figures 5.4 and 5.5 the interpretation of the CFD-results is based on the rendering of the pressure distribution and velocity field of the fine grid. While the coarse mesh resolution shows some significant changes in the flow field the standard and fine grid demonstrate almost equal results. The most significant changes appear in the sizes and the exact locations of the vertices. This is caused by the varying resolution of the grid itself. While the occurrences of vertices from the standard and fine mesh show almost no differences in location, the sizes do fluctuate between the two resolutions.

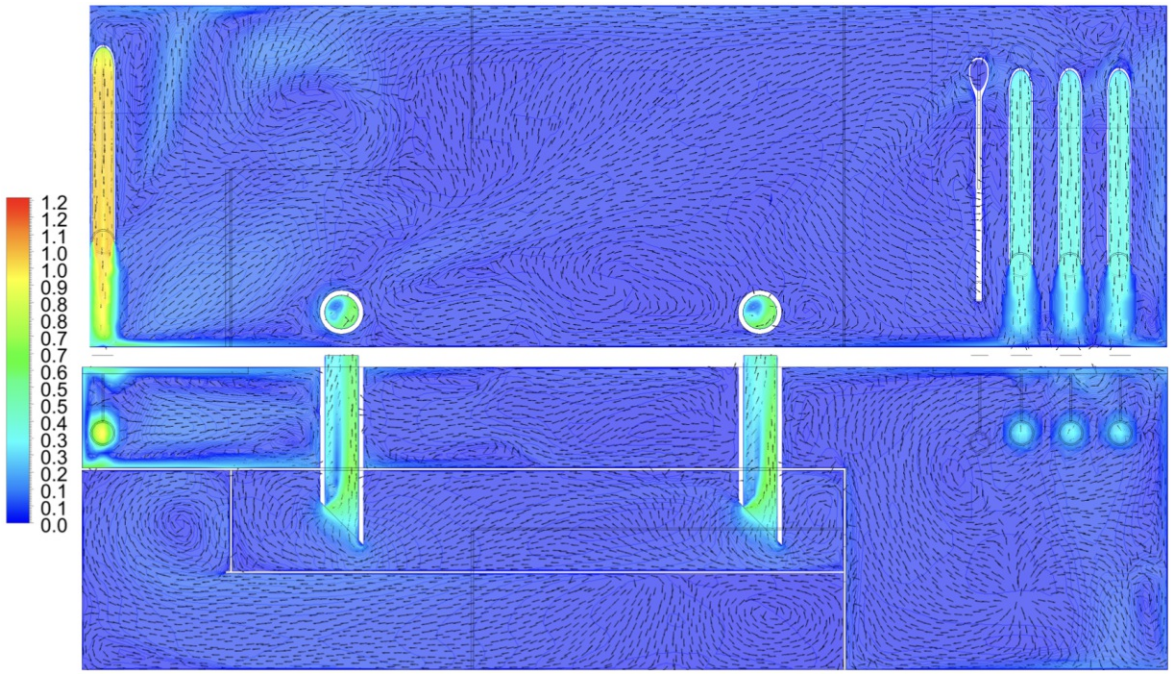

Figure 5.4 – Contour plots of flow field illustrated with a normalisation coefficient of 10 $\frac{m}{s}$: top image represents a vertical cut through the hydraulic tank right underneath the inlet pipes; the bottom one shows the velocity field of a horizontal cut through the outlet pipes

A closer look at the normalised flow fields of figure 5.4 reveals the details of two different planes through the hydraulic reservoir. The plot right through all the active pipes highlights that the inlet-condition of the pipe on the left has a major impact on the flow situation in the region between the outer structure and the first baffle parallel to the cutting plane. These high velocities at the inlet determine the formation of vertices in this flow area, compared contour plots in figure 5.4. The impacts of the inlet pipes on the right side are also displayed in figure 5.4. Due to the shape of the pipes the inlet stream creates vertices perpendicular to the image plane. This behaviour may lead to issues of the air separating capacity, foam formation and particle sedimentation. As it is illustrated in figure 5.4 the right use and arrangement of thin baffles helps to slow down the hydraulic medium and regain its properties. In the last remaining flow regions only two slightly larger vertices appear. This behaviour is traced back to the shape of the hydraulic reservoir and the locations of the baffles itself. As shown in figure 5.4 those vertices are located in calmed areas right next to the solid structure and do not have as much influence on the above mentioned issues as it is the case at the inlet regions. Another essential quantity to describe the flow state of the hydraulic reservoir is the pressure distribution over different planes. The data displayed in the

contour plot of figure 5.5 highlights the locations of the pressure maxima and points out the low pressure regions at the suction pipes. The reference value to normalise the pressure as it is given in figure 5.5 is 1 *bar*.

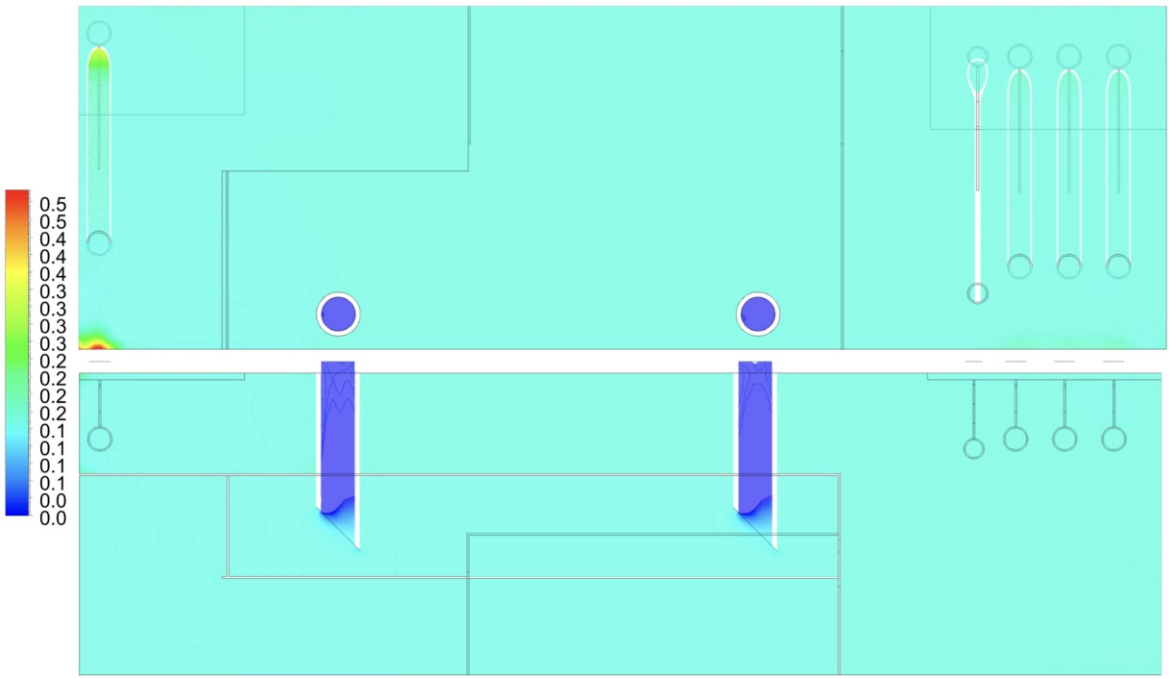

Figure 5.5 – Contour plot of the pressure distribution at two characteristic planes: top image represents a vertical cut through the hydraulic tank right underneath the inlet pipes; the bottom one illustrates the pressure field at the suction pipes

Besides all the provided information of the flow field contour plots the analysis of other physical quantities like pressure at distinct locations is vital for improvements of the layout. In this research work normalised pressure plots over a distinct location are compared with each other. The value of the normalising coefficients are 10 *bar* for the pressure and 100 *mm* for the length coordinate. As given in figure 5.6 the pressure profiles are plotted over a cut through the hydraulic reservoir in a parallel direction of the inlet pipe's orientation (cross section). This chart represents the pressure difference between the induced pressure of the inlet stream and the predominating pressure at the bottom plate of the hydraulic tank. The profiles of figure 5.6 represent the pipes according to figure 5.4 starting from the left inlet pipe. The noticeable peculiarities of figure 5.6 are the very tight peaks of the left chart. Those peaks represent the pressure changes caused by the baffle close to the inlet pipe. The maximum of this pressure profile can be referred to the high inlet velocity stream of the feeding pipe

which corresponds to a stagnation point. This leads to an increase in pressure right underneath the pipe's surface area, compare figure 5.6. The other chart in figure 5.6 represents the behaviour for the first feeding pipe of the inlet triplet on the right side of figure 5.4. As it is illustrated the induced pressure on the bottom of this inlet pipe is approximately three times less than it is the case of the left chart in figure 5.6. This is due to the lower velocity at the inlet.

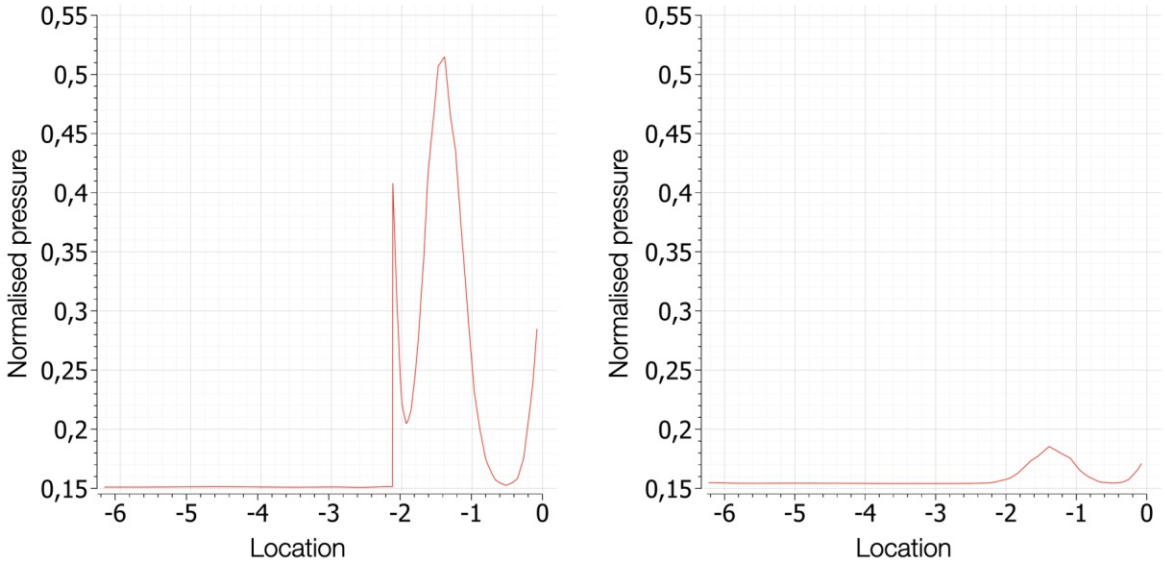

Figure 5.6 – Normalised pressure profile of the inlet pipes (reference values 10 *bar* and 100 *mm*): the chart on the left shows the pipe with the highest inlet velocity value; the chart on the right represents the left inlet pipe of the triplet of tubes

The data illustrated in figure 5.7 corresponds to the pressure profiles of the remaining two inlets of the pipe triplet. As it is shown the characteristic peaks of those curves are almost identical and have the same progression as the first pipe of this group of tubes. Besides a detailed view of each inlet an overview of all feeding pipes points out the correlations between them. The profile given in figure 5.8 illustrates the changes of pressure over the longitudinal extension of the hydraulic reservoir in x-direction. Again the reference values of the normalised pressure and length coordinate are 10 *bar* and 100 *mm*. As illustrated there are four characteristic peaks, which do refer to the same sequence and locations of the feeding pipes as it is displayed in figure 5.4. The pressure profile of figure 5.8 is a good validation for the curves of figures 5.6 and 5.7. Those curves do only differ on the chosen plane of the presentation of the pressure profiles.

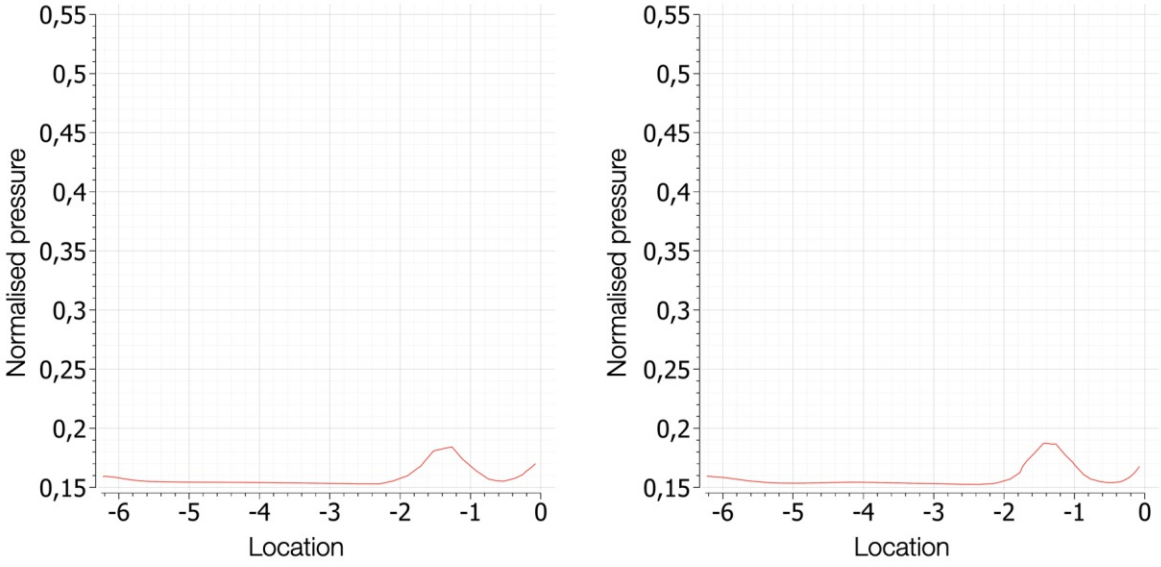

Figure 5.7 – Normalised pressure profile of the inlet pipes (reference values 10 bar and 100 mm): the charts represent the pressure curve of the remaining two pipes of the triplet in the same order as it is illustrated in the velocity field plots

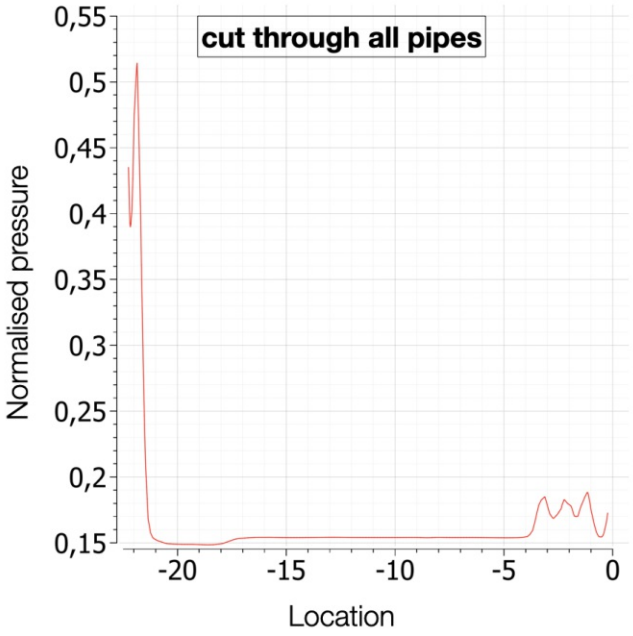

Figure 5.8 – Normalised pressure profile of all active inlets (reference values 10 bar and 100 mm): pipes are displayed in the same sequence as in the velocity field contour plots

6

Novel diffuser design analysis

One good test is worth a thousand expert opinions.

Wernher von Braun

6.1 Shape & design

Most common practice of industry pipes are a straight line design. This may often not only lead to issues of the mechanical structure but also to randomly disturbed flow patterns and swirling. An approach to reduce these problems are new innovative inlet layouts, e.g. diffusers [1]. In this research work a particular diffuser design in various configurations is investigated. This study should illustrate the advantages of the use of such a novel inlet layout. In total four slightly different axis-symmetrically drafts are investigated and compared. The basic design of this diffuser consists of steel plates and tapered holes in the centre of these metal sheets, shown in figure 6.1. For the simplification of the CFD-analysis the bolts which hold the round metal sheets in place are removed. The layouts only differ in the spacing between the steel plates and the ratio of the conical cut outs of the metal sheets. These steel plates have a thickness of a few millimetres and a diameter of around 23 times the plate thickness. The significant differences of the geometry are shown in figures 6.3, 6.4. The main objective of the use of a diffuser is to reduce mechanical stresses on the structure, pipes, decrease swirling and slow down the flow field inside the tank.

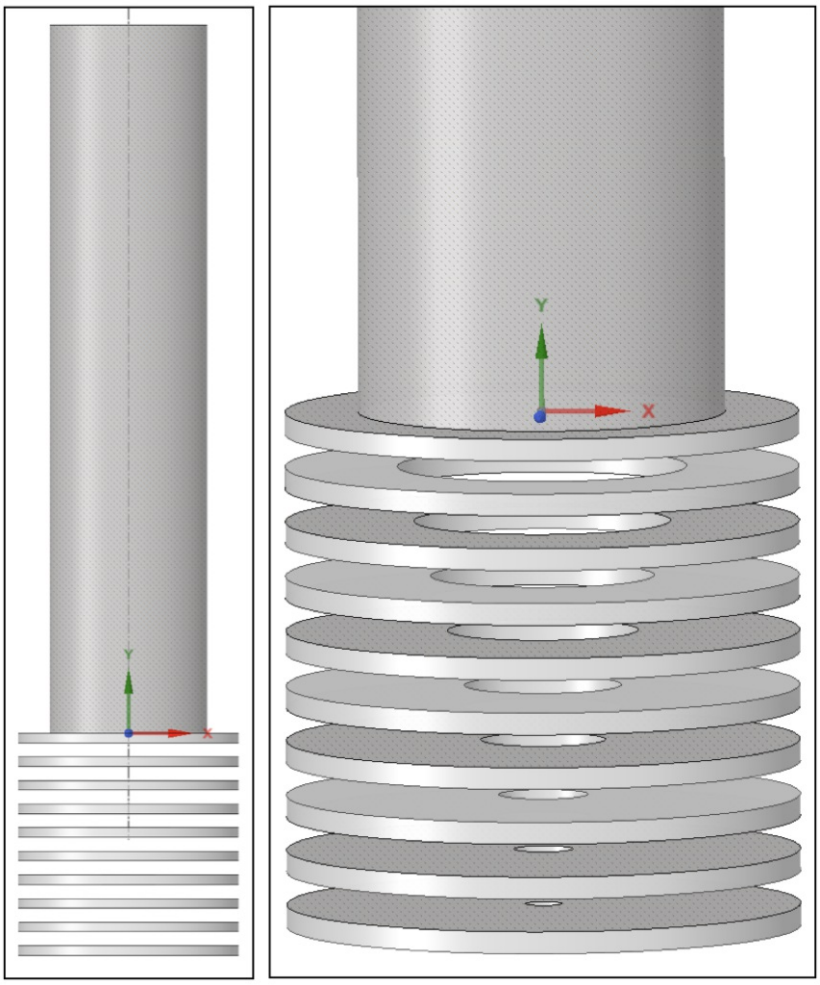

Figure 6.1 – Basic diffuser geometry layout without bolts to reduce the computational effort of the CFD - simulation

6.2 Mesh

The mesh for the various diffuser designs are all computed in *ANSYS Meshing* and are two dimensional compared to the hydraulic reservoir ones. The number of elements differ a little bit, depending on the actual layout of the spacing between the steel plates. For the configurations with a larger spacing between the metal sheets less flow elements are used. The general information about the mesh sizes of the four layouts are given in table 6.1. Refinements of the mesh are made at the inlet, steel plates and outlet regions. This includes element sizing between the metal sheets with the tapered cut outs and along the inlet pipe. To gather detailed information about the velocity gradients, a total number of four inflation layers are added to the steel plates of the diffuser. The maximum element size is set to a maximum value of 10 mm for all four layouts.

		Number of elements
Mesh	Design I	31 149
	Design II	30 114
	Design III	31 396
	Design IV	30 865

Table 6.1 – Number of elements of diffuser designs

6.3 General setup of the simulation

The study of different diffuser inlet designs are carried out as an axially symmetric two dimensional problem formulation. This simplification from a three dimensional problem to a two dimensional one helps to reduce the computational time tremendously. The CFD analysis consists only of the investigation of the diffuser and the surrounded walls without the interactions inside the hydraulic tank taken into account.

6.3.1 Selected Models

There are a few differences to the simulation set up of the investigation of the diffuser layouts compared to the hydraulic reservoir. First of all the four diffuser designs are an axially symmetric two dimensional problem. Secondly only the SST k-ω model without any changes to the one used for the hydraulic tank is applied. Only alterations of the flow field without any temperature changes are of interest.

6.3.2 Boundary Conditions

The boundary conditions are similar to the ones of the hydraulic reservoir since the same inlet flow state is of interest. Changes are only made to the conditions of the surrounded walls since those are the only parts which were modified compared to the hydraulic tank. These changes are important because only the diffuser inlet part itself is investigated and not the fully assembled hydraulic reservoir. For the CFD analysis there are exactly four types of boundary conditions: one velocity inlet, one pressure outlet, one axis-symmetric and no slip wall conditions. All values are given in table 6.2.

		Type
Boundary cond.	Inlet	velocity-inlet
	Outlet	pressure-outlet
	Wall	stationary/no slip
	Axis	axissymmetric

Table 6.2 – Boundary conditions of the CFD analysis of the different diffuser designs

6.3.3 Methods & Controls

The general setup of the CFD analysis is a pressure-based steady simulation. As it is the case of the hydraulic reservoir also gravitational effects are taken into account. Compared to the default settings changes in the discretization schemes are made. All approaches of the gradient, pressure, momentum, turbulent kinetic energy and specific dissipation rate are set to second order. A pseudo transient formulation and the warped-face gradient correction are enabled to obtain realistic data about the flow situation. The controls of the explicit relaxation factors for the pseudo transient simulation are set to the default values as the convergence behaviour of the residuals and some physical quantities are fulfilled. All values for pressure, momentum, density, body forces, turbulent kinetic energy, specific dissipation rate and turbulent energy are given in table 6.3.

		Values
Explicit Relaxation Factors	Momentum	0.5
	Pressure	0.5
	Density	1
	Body Forces	1
	Turbulent kinetic energy	0.75
	Specific dissipation rate	0.75
	Turbulent viscosity	1

Table 6.3 – Explicit relaxation factors of diffuser CFD analysis

6.4 CFD - Analysis

All residuals and some physical quantities, e.g. pressure at outlet, have been converged for all four diffuser designs. Further details of the convergence behaviour are shown in the appendix according to A.2.

		Convergence criteria
Residuals	Continuity	$< 10^{-3}$
	x-velocity	$< 10^{-5}$
	y-velocity	$< 10^{-5}$
	k	$< 10^{-5}$
	ω	$< 10^{-5}$
	pressure at outlet	$< 10^{-3}$
	velocity at outlet	$< 10^{-3}$

Table 6.4 – Convergence criteria for 2D CFD analysis of diffuser designs

6.4.1 Results

In general the convergence criteria is based on a practical approach of the industry. Therefore the conditions for the various diffuser designs are given in table 6.4. These conditions must be fulfilled to obtain proper CFD results.

The results of the CFD-analysis can be divided into two categories. The first one as the examination of the flow field and its changes due to the adaption of the diffuser's geometry. The second category concerns the investigation of changes of other physical quantities, e.g pressure or wall shear stress. Both categories are thoroughly discussed in this section. First, a closer look on the flow field patterns of the different inlet designs reveals that the critical changes depend on the spacing between the steel plates and on the bottom plate of the diffuser. The scale of the velocity magnitude is a normalised one. Therefore, all given velocity values are referred to a reference velocity of 10 $\frac{m}{s}$.

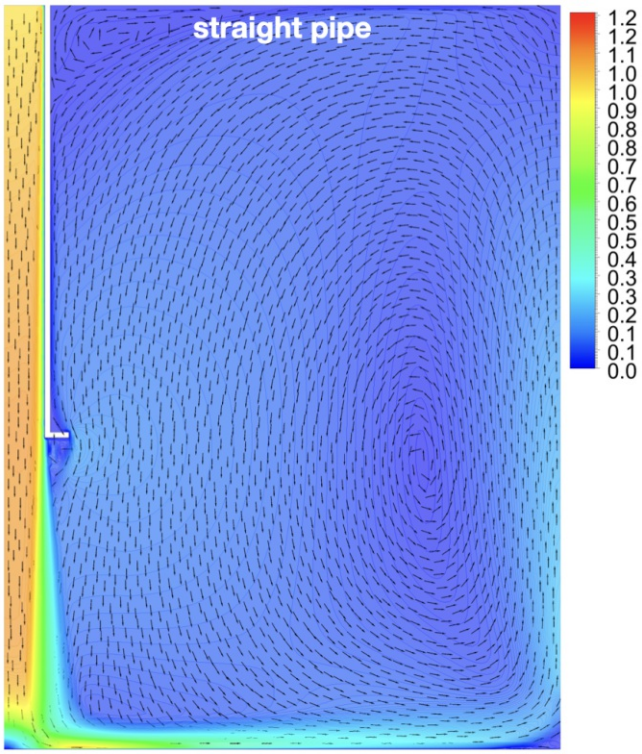

Figure 6.2 – Contour plot of the flow field of the straight inlet pipe design; all velocity values are normalised with a reference velocity of 10 $\frac{m}{s}$

Major changes of the flow field compared to the original configuration consist of the size and formation of vertices. The comparison of the design I and II, shown in figure 6.3, highlights the differences in size of vertices and the deflection of the hydraulic medium caused by the metal plates. This deflection of the inlet stream does strongly depend on the spacing between the steel sheets, as it is shown in figures 6.3, and 6.4. The same analogy is valid for design III and IV. Only the distance between the metal plates of design IV is less than for the layout II. Configurations I and III have the exact same spacing between the sheets. As shown in figure 6.4 the third and fourth designs exhibit the smallest vertex right underneath the bottom plate of the diffuser. This critical change in the layout of the diffuser's last plate does affect the flow field essentially. Beside this formation of vertices underneath the diffuser, the inlet stream is less deflected than it is the case for an open bottom plate of design I and II. This results in the assumption of less swirling within the hydraulic tank if such diffuser designs are assembled to the inlet pipes. One similarity of all diffuser configurations is the appearance of the highest stresses on the plates. Those stresses occur on the inside tips of the steel plates as illustrated in figures 6.3, 6.4. As given in figures 6.6 and 6.7 the

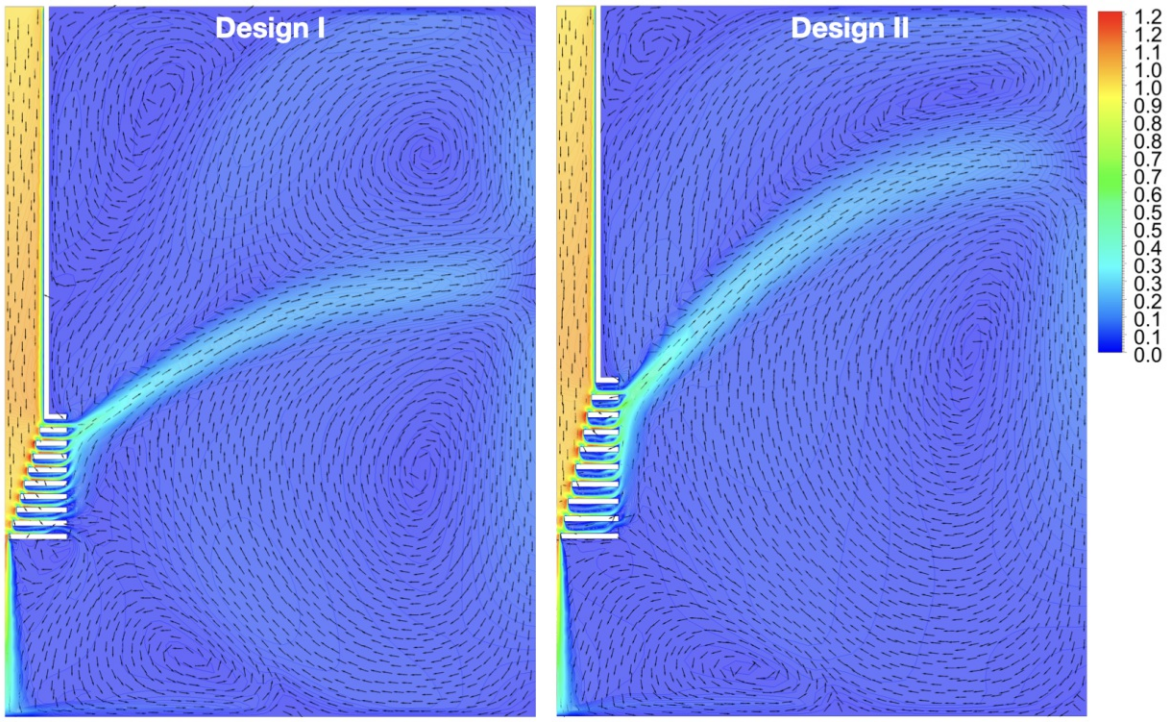

Figure 6.3 – Contour plot of the flow fields of design I & II with a cut out in the bottom diffuser plate;all velocity values are normalised with a reference velocity of 10 $\frac{m}{s}$

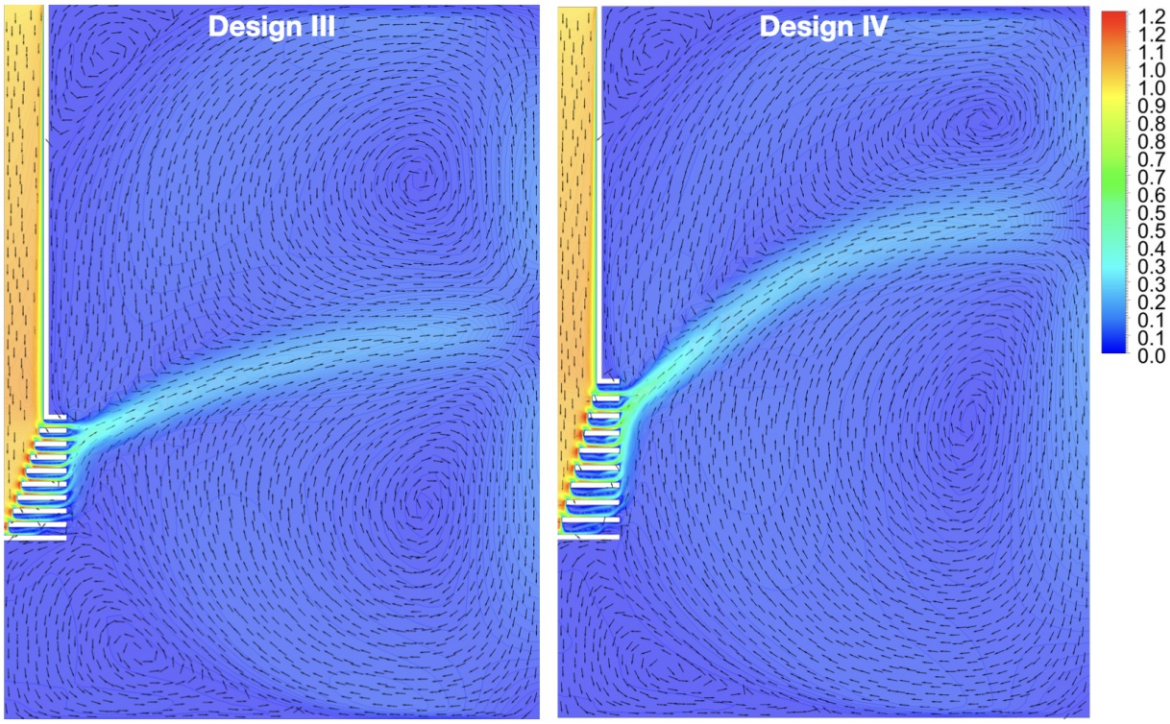

Figure 6.4 – Contour plot of the flow field of design III & IV without a hole in the bottom diffuser plate;all velocity values are normalised with a reference velocity of 10 $\frac{m}{s}$

maximum average pressure over the inlet surface occur at the diffuser designs with less spacing between the metal plates. This has to be considered if a novel diffuser layout is applied to the given inlet configuration because these higher pressure arises from the dispersive task of a diffuser.

The second major category of this investigation of different inlet configurations is an in-depth view on a physical quantity. Therefore, the pressure profiles at specific locations of the hydraulic container, e.g. at the inlet and at the bottom, are observed. The y-axis represents the normalised pressure and the x-axis illustrates the normalised length coordinate at which the pressure is plotted. The reference value for the pressure is $1\,bar$ and the coordinate of the location is referred to $100\,mm$.

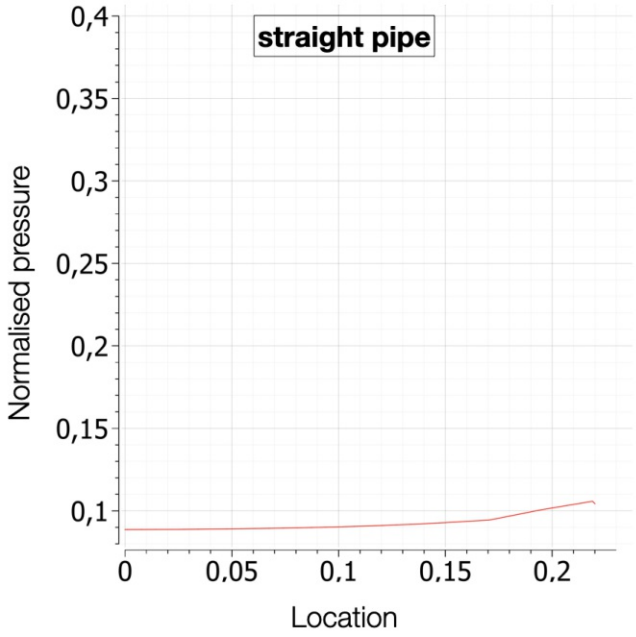

Figure 6.5 – Pressure curves of the straight pipe design at the inlet with an average pressure of $0,01\,bar$

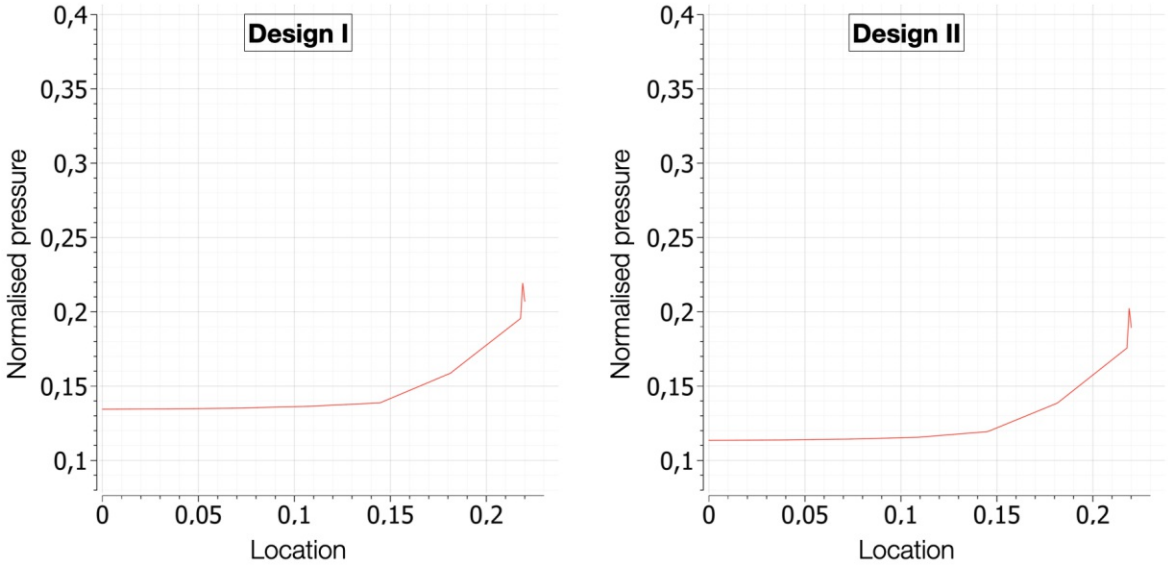

Figure 6.6 – Pressure curves of designs I & II at inlet with an average pressure of $0,15\,bar$ for layout I and $0,13\,bar$ for design II

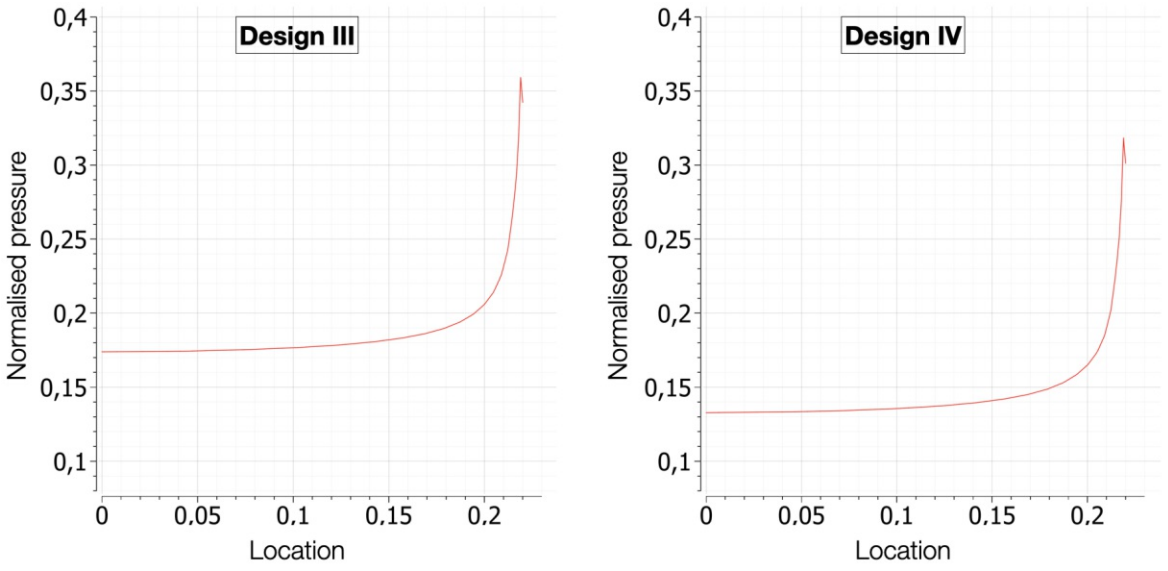

Figure 6.7 – Pressure curves of designs III & IV at inlet with an average pressure of $0,19\,bar$ for layout III and $0,15\,bar$ for design IV

As it is shown in figures 6.5, 6.6, 6.7, the curves of the pressure at the inlet appear to have the same development but do vary in the average inlet pressure values. This is a consequence of the different inlet respectively diffuser designs. The experimental data shows the lowest pressure values at the straight pipe layout. This behaviour is due to the lack of a diffusive device. Other curves are obtained if the pressure on the bottom plate is plotted, compare figures 6.8, 6.9, 6.10. As assumed the curves do differ between the designs of a straight pipe, a diffuser with a cut out at the final plate and

the configurations without a hole in the last plate. Notable is the occurrence of almost zero pressure at the bottom of the test reservoir for designs III & IV, given in figure 6.10. As a consequence the more the inlet stream is deflected by a diffusive device, less stresses act on the bottom of the hydraulic tank. The comparison of the straight pipe layout with the designs I & II shows a dramatically reduction of pressure acting on the outer structure even if the configuration of the diffuser has a cut out in its plate arrangement, shown in figure 6.8, 6.9. This straight inlet pipe design has a ten times higher pressure stress on the bottom structure than it is the case for the alternative diffuser configurations.

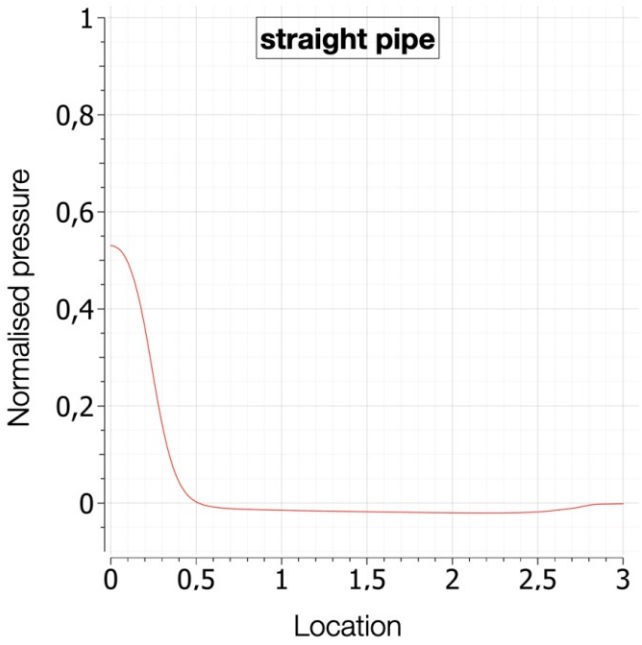

Figure 6.8 – Normalised pressure profiles of the straight pipe design on the bottom plate

The major differences between the plotted curves 6.8 and 6.10 remain the stagnation pressure right underneath the diffuser plate with the cut out and also the magnitude of the pressure acting on the bottom of the reservoir. The amplitude of the pressure do strongly depend on the geometry of the inlet layout itself. As illustrated in figures 6.8, 6.9 and 6.10 the magnitude is much higher for the open bottom plate design.

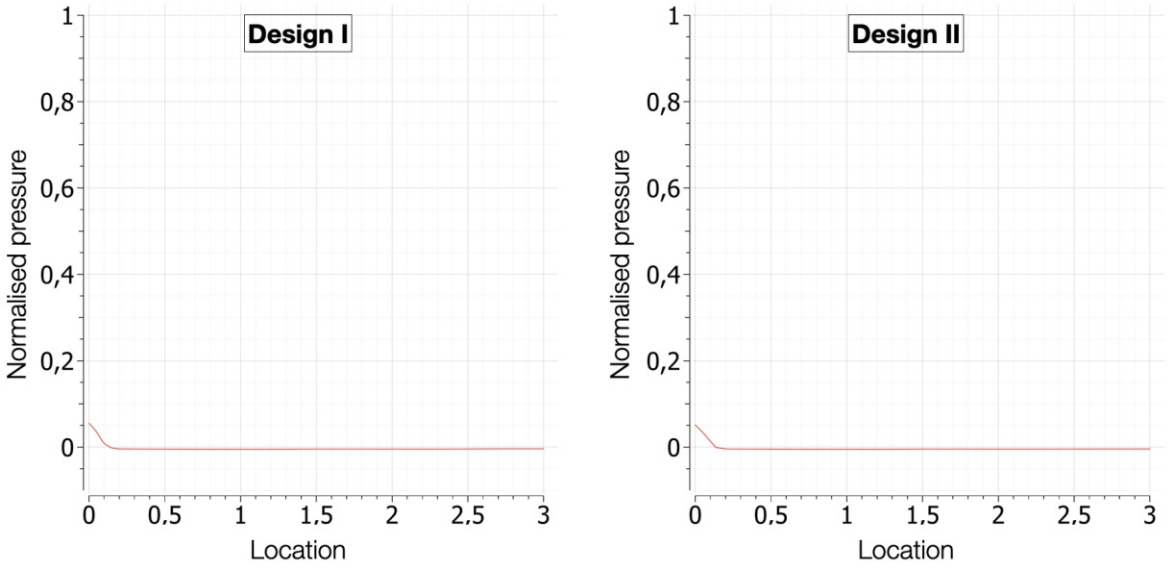

Figure 6.9 – Normalised pressure profiles of the diffuser designs I & II at the bottom plate

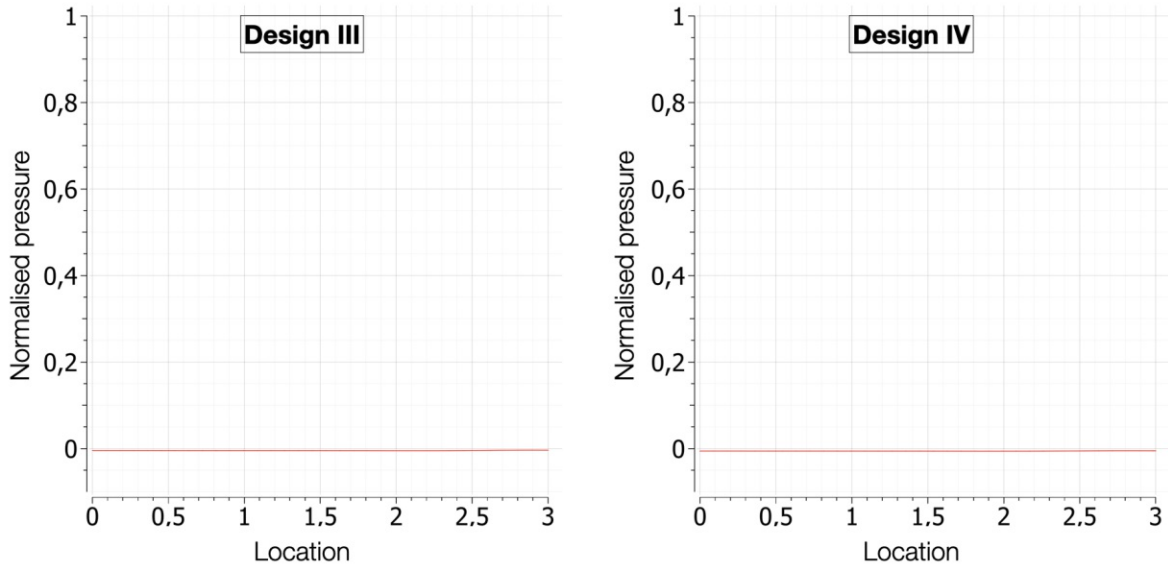

Figure 6.10 – Normalised pressure profiles of the diffuser designs III & IV at the bottom plate

7

Conclusion

In the middle of difficulty lies opportunity.

Albert Einstein

To sum everything up the right choice of the layout of the hydraulic structure is key to a proper operating hydraulic power unit. Frequently quite conservative hydraulic reservoir designs are found in industry and literature of which almost all possess the same issues.

The simulations carried out in this research work ought to highlight the role of different inlet designs and the resulting consequences. As the current state of the hydraulic reservoir has been presented with the means of CFD simulations, an alternative novel diffuser design has been thoroughly studied and compared to the given situation. The investigated diffuser layout could lead to a reduction of mechanical stress on the outer structure when it is applied properly to the hydraulic reservoir. This does not only result in a weight reduction of the whole system at all but also gives rise to a harmonisation of the flow field due to the separation of the inlet stream. The results of the diffuser designs look promising to withstand the mechanical stresses and are a developable alternative to the conservative inlet design of the last decades in the industry. Further analysis of the spacing between the plates must be carried out to find the ideal distance for less swirling.

Nevertheless to develop an efficient and proper working inlet diffuser for a hydraulic reservoir is not as simple as it may appear at the first sight. Many aspects of this complex issue must be taken into account to identify the ideal design for its application. As this development process is an iterative one a combination of both, a CFD and a FEA analysis is recommended. With these little changes in hardware magnificent improvements of the efficiency of a hydraulic power unit will follow.

Bibliography

[1] V. Tič and D. Lovrec, "Design of Modern Hydraulic Tank Using Fluid Flow Simulation," *International Journal of Simulation Modelling*, vol. 11, no. 2, pp. 77–88, 2012.

[2] J. Gorle, "Coupled Fluid-Thermal-Structural Analysis of Two-Phase Flow in a Hydraulic Tank," no. May, 2019.

[3] N. Belov and N. Sosnovsky, "Design of an Optimal Hydraulic Tank Configuration," *IOP Conference Series: Materials Science and Engineering*, vol. 779, no. 1, 2020.

[4] V. Singal, J. Bajaj, N. Awalgaonkar, and S. Tibdewal, "CFD Analysis of a Kerosene Fuel Tank to Reduce Liquid Sloshing," *Procedia Engineering*, vol. 69, pp. 1365–1371, 2014.

[5] C. Zhang, "Application of an Improved Semi-Lagrangian Procedure to Fully-Nonlinear Simulation of Sloshing in Non-Wall-Sided Tanks," *Applied Ocean Research*, vol. 51, pp. 74–92, 6 2015.

[6] J. Untch, "Capabilities and Challenges of CFD in Multiphase Simulation of Hydraulic Tanks," vol. 1, pp. 1–7, 2014.

[7] M. Močilan, M. Žmindák, P. Pecháč, and P. Weis, "CFD Simulation of Hydraulic Tank," *Procedia Engineering*, vol. 192, pp. 609–614, 2017.

[8] V. Tič and D. Lovrec, "Air-Release and Solid Particles Sedimentation Process within a Hydraulic Reservoir," *Tehnički vjesnik*, vol. 20, no. 3, pp. 407–412, 2013.

[9] A. Wohlers, A. Backes, and D. Schönfeld, "An Approach to Optimize the Design of Hydraulic Reservoirs," *10th International Fluid Power Conference (IFK2016)*, pp. 609–618, 2016.

[10] L. Muttenthaler, *Analytische , numerische und experimentelle Untersuchungen von Feststoffverschmutzungen in hydraulischen Systemen.* PhD thesis, 2020.

[11] A. Osmanović, A. Efendić, and E. Trakić, "Modelling, Optimal Design and Simulation of Hydraulic Oil Reservoir," vol. 17, pp. 33–46, 2019.

[12] L. Muttenthaler and B. Manhartsgruber, "Prediction of Particle Resuspension and Particle Accumulation in Hydraulic Reservoirs Using Three-Phase CFD Simulations," in *ASME/BATH 2019 Symposium on Fluid Power and Motion Control*, American Society of Mechanical Engineers, 10 2019.

[13] L. Muttenthaler and B. Manhartsgruber, "Euler–Lagrange CFD simulation and experiments on accumulation and resuspension of particles in hydraulic reservoirs," *Journal of the Brazilian Society of Mechanical Sciences and Engineering*, vol. 42, no. 4, 2020.

[14] A. Busch and J. Gottschang, "Ölbehälter - Optimierung für die Zukunft," 2015.

[15] G. Dimmler, J. Kilian, P. Bader, L. Muttenthaler, and P. Kapeller, "So That the Heart of the Machine Beats Longer," *Kunststoffe International*, vol. 108, no. 10, pp. 56–59, 2018.

[16] L. Muttenthaler and B. Manhartsgruber, "Optimizing Hydraulic Reservoirs Using Euler-Euler-Lagrange Multiphase CFD Simulation," pp. 295–304, 2020.

[17] M. Singh, G. S. Lathkar, and S. K. Basu, "Failure Prevention of Hydraulic System Based on Oil Contamination," *Journal of The Institution of Engineers (India): Series C*, vol. 93, no. 3, pp. 269–274, 2012.

[18] H. D. Baehr and S. Kabelac, *Thermodynamik*. Springer-Lehrbuch, Berlin, Heidelberg: Springer Berlin Heidelberg, 2012.

[19] G. E. Totten, *Handbook of Hydraulic Fluid Technology*. CRC Press, 10 2011.

[20] D. Findeisen and S. Helduser, *Ölhydraulik*. Berlin, Heidelberg: Springer Berlin Heidelberg, 2015.

[21] D. Will and N. Gebhardt, eds., *Hydraulik*. Berlin, Heidelberg: Springer Berlin Heidelberg, 2014.

[22] M. Longhitano, A. Protase, and H. Murrenhoff, "Experimental Investigation of the Air Release in Hydraulic Reservoirs," *10th International Fluid Power Conference (IFK2016)*, pp. 597–608, 2016.

[23] S. Sakama, Y. Tanaka, and H. Higashi, "Air Bubble Separation and Elimination from Working Fluids for Performance Improvement of Hydraulic Systems Air Bubble Separation and Elimination from Working Fluids for Performance Improvement of Hydraulic Systems," no. August 2015, 2014.

[24] C. Jensen, *Clean Oil Guide*. Svendborg, Denmark: C. C. Jensen A/S, ver. 011 ed., 2019.

[25] D. L. Douglass, "Understanding Truck Mounted Hydraulic Systems," tech. rep., Muncie Power Products, Inc., Muncie, Indiana, 2006.

[26] C. L. Zhao and R. Schiffers, "Condition monitoring of non-return valves in injection molding machines using available process and machine data," in *AIP Conference Proceedings*, vol. 2205, 2020.

[27] F. Ng, J. A. Harding, and J. Glass, "Improving Hydraulic Excavator Performance Through in Line Hydraulic Oil Contamination Monitoring," *Mechanical Systems and Signal Processing*, vol. 83, pp. 176–193, 2017.

[28] R. Garvey and G. Fogel, "Converting Tribology Based Condition Monitoring Into Measureable Maintenance Results," 1998.

[29] A. G. Elkafas, M. M. Elgohary, and A. E. Zeid, "Numerical study on the hydrodynamic drag force of a container ship model," *Alexandria Engineering Journal*, 2019.

[30] R. A. Ibrahim, *Liquid Sloshing Dynamics*. Cambridge University Press, 5 2005.

[31] J. Novak-Marcincin, P. Brazda, M. Janak, and M. Kocisko, "Application of Virtual Reality Technology in Simulation of Automated Workplaces," *Technical Gazette*, vol. 18, no. 4, pp. 577–580, 2011.

[32] J. M. Gorle, B. F. Terjesen, A. B. Holan, A. Berge, and S. T. Summerfelt, "Qualifying the Design of a Floating Closed-Containment Fish Farm Using Computational Fluid Dynamics," *Biosystems Engineering*, vol. 175, pp. 63–81, 2018.

[33] J. M. Gorle, B. F. Terjesen, and S. T. Summerfelt, "Hydrodynamics of Octagonal Culture Tanks with Cornell-Type Dual-Drain System," *Computers and Electronics in Agriculture*, vol. 151, no. February, pp. 354–364, 2018.

[34] J. M. Gorle, L. Chatellier, F. Pons, and M. Ba, "Operation of Darrieus Turbines in Constant Circulation Framework," *Physics of Fluids*, vol. 29, no. 7, 2017.

[35] A. W. Patwardhan, "CFD Modeling of Jet Mixed Tanks," *Chemical Engineering Science*, vol. 57, no. 8, pp. 1307–1318, 2002.

[36] L. Hou, F. Li, and C. Wu, "A numerical study of liquid sloshing in a two-dimensional tank under external excitations," *Journal of Marine Science and Application*, vol. 11, no. 3, pp. 305–310, 2012.

[37] H. Kuhlmann, *Strömungsmechanik*. Hallbergmoos: Pearson Deutschland GmbH, 2014.

[38] A. Inc., "ANSYS Fluent Theory Guide," tech. rep., Canonsburg, PA, US, 2021.

[39] F. R. Menter, "Two-equation eddy-viscosity turbulence models for engineering applications," *AIAA Journal*, vol. 32, pp. 1598–1605, 8 1994.

[40] D. C. Wilcox, *Turbulence modeling for CFD : [Hauptbd.]*. La Canada, Calif: DCW Industries, 2. print. (with c... ed., 1994.

[41] R. Doddannavar and A. Barnard, *Practical hydraulic systems : operation and troubleshooting for engineers and technicians*. Practical professional books from Elsevier, Oxford: Newnes, 2005.

[42] LUKOIL Lubricants Europe GmbH, "LUKOIL GEYSER ST - DATASHEET," tech. rep., Vienna, 2018.

[43] A. Banaszek and R. Petrović, "Calculations of the Unloading Operation in Liquid Cargo Service with High Density on Modern Product and Chemical Tankers Equipped with Hydraulic Submerged Cargo Pumps," *Strojniski Vestnik/Journal of Mechanical Engineering*, vol. 56, no. 3, 2010.

[44] PCC Rokita SA, "ROKOLUB P-46VI - DATASHEET," tech. rep., Brzeg Dolny.

[45] PCC Rokita SA, "Industrial Fluids and Lubricants Base Stocks," tech. rep., Brzeg Dolny.

[46] M. J. Neale and D. Harrison, "The Tribology handbook," *Choice Reviews Online*, vol. 33, no. 11, pp. 33–6332, 1996.

[47] A. Inc., "ANSYS Fluent User's Guide," tech. rep., Canonsburg, PA, US, 2021.

List of Figures

List of Tables

A

Appendix

A.1 Oil data sheets

Further properties of the *Lukeoil Geyser ST 46* are given in the data sheets below. The used mineral oil *Lukeoil Geyser ST 46* corresponds to the *type 46* of the ISO classification system.

LUKOIL GEYSER ST

PRODUKTNUMMER: 572530

hochwertige Hydrauliköle für schwer belastete Hydraulikanlagen

FREIGABEN

Bosch Rexroth RD90220
Parker Denison HF-0
PALFINGER
Thyssenkrupp (ISO VG 32, 46, 68)

SPEZIFIKATION & QUALITÄTSNIVEAU

DIN 51524-2 HLP
ISO 6743-4 HM
US Steel 127/136
VDMA 24318 – HLP
Eaton Brochure 03-401-2010 (ersetzt Vickers I-286-S & M-2950-S)
JCMAS HK
GM LS-2
Cincinnati P68/69/70

Schadenskraftstufe **DIN ISO** 14635-1 A/8,3/90-M:>10

PRODUKT BESCHREIBUNG

Öle der Serie **LUKOIL GEYSER ST** zeigen günstiges Viskositäts-Temperaturverhalten, hervorragende Alterungsstabilität und wirksamen Korrosionsschutz. Besondere Zusätze verbessern das Verhalten im Mischreibungsbereich, wodurch niedrige Verschleißwerte erreicht werden.

Öle der Serie **LUKOIL GEYSER ST** besitzen geringe Schaumneigung, gutes Luftabscheide- und Demulgiervermögen und verhalten sich neutral gegenüber handelsüblichen Dichtungswerkstoffen.

ANWENDUNG

Vorwiegend in stark beanspruchten hydrostatischen Anlagen nach Herstellervorschrift. Öle der Serie **LUKOIL GEYSER ST** eignen sich dank der Verschleißschutzeigenschaften auch als Schmieröl für Stirnradgetriebe oder als Umlaufschmieröl für Gleit- und Wälzlager. Die Herstellervorschriften sind zu beachten!

Falls noch besseres Viskositäts-Temperatur-Verhalten vorgeschrieben oder gewünscht wird, verweisen wir auf unsere Mehrbereichshydrauliköle der **LUKOIL GEYSER M** Reihe.

TECHNISCHE DATEN

EIGENSCHAFT	Einheit	Testmethode	LUKOIL GEYSER ST					
			10	22	32	46	68	100
Dichte bei 15°C	kg/m³	DIN 51757	844	838	875	878	882	885
Flammpunkt COC	°C	ISO 2592	>140	>210	>210	>210	>210	>210
Viskositätsklasse	---	ISO VG	10	22	32	46	68	100
Viskosität bei 40°C	mm²/s	DIN 51562/T1	10	22	33	46	69	101
Viskosität bei 100°C	mm²/s	DIN 51562/T1	2,7	4,6	5,5	6,8	8,7	11,2
Viskositätsindex	--	DIN ISO 2909	108	127	102	101	99	97
Pourpoint	°C	DIN ISO 3016	<-39	<-24	<-24	<-24	<-24	<-18

Die angeführten Informationen unter den technischen Daten stellen keine Spezifikation dar, sondern sind ein Hinweis aus der gegenwärtigen Produktion und diese können zulässigen Herstellungstoleranzen unterliegen. OOO „LLK-International“ behält sich das Recht auf Änderungen vor.

Weitere Auskünfte erhalten Sie vom technischen Marketing Service Schmierstoffe unter technics.lubes@lukoil.com

LUKOIL Lubricants Europe GmbH
Uferstrasse 8
1220 Vienna, Austria

+43(1)205 222-8800
www.lukoil-lubricants.eu

ROKOLUB P-46VI

CHEMICAL NAME	Polyether polyol
CAS NUMBER	74499-34-6
TECHNICAL REQUIREMENTS	Appearance at (25 ℃)….. Homogenous, colorless to yellow liquid Water content, % (m/m)……..….max. 0.1 ASTM D4672-12 Acid value, mg KOH/g……..max. 0.1 ASTM D7253-06(2011), Kinematic viscosity at 40°C, cSt….43 – 53 ASTM D445-15 Kinematic viscosity at 100°C, cSt…. 8,5 – 10,5 ASTM D445-15
GENERAL DATA	ISO VG 46 Molecular weight, g/mol ~900 Viscosity index ~182 Pour point, ℃ -43 Flash point, ℃ ~243
APPLICATION	Rokolub P-46VI is a product with high Viscosity Index, insoluble in water, applied as PAG synthetic base oil. Applications: Lubricating oil for industrial gears and compressor, as a hydraulic and metalworking fluids.

PCC Rokita SA
ul. Sienkiewicza 4
56-120 Brzeg Dolny
Poland

MOL Thermol 46

heat transfer oil

MOL Thermol 46 is a mineral oil based heat transfer oil having high viscosity index and narrow boiling point range. The allowed maximum film temperature at the heat transfer surface is 350 °C, and in the system it is 330 °C.

The service life of the heat transfer medium depends greatly on the design of the heat transfer system and on the operating conditions. The service life could be up to 5 years, if the system is designed properly, and when it is protected from extreme load conditions. The service life could be extended significantly if low pressure (1.2 - 1.5 bar gage pressure) inert gas atmosphere (nitrogen) is used in an expansion tank.
For safety and economic reasons, it is recommended to check the condition of the oil on a regular basis, but once a year at least.
Handling MOL Thermol 46 is safer than when handling most other synthetic oils, as it is not toxic and has a low vapour pressure. It can be collected as used oil after its application, for recycling or disposal.

The physical properties considered to be important in terms of heat transfer are collected in a separate table, as a function of the temperature.

Application

	Closed circuit heat transfer systems with indirect heating and forced circulation

Features and benefits

Excellent thermal stability	Resists thermal decomposition and deposit formation in the long term, even at high operating temperatures Extended trouble-free operation, so less downtime Low maintenance cost
Long oil lifetime	Oil change and reconditioning costs can be reduced significantly
Excellent thermal properties	Effective heat transfer between surfaces Improved efficiency, giving reduced operational costs
Good corrosion protection	Long-term protection of steel and non-ferrous metal parts
Compatible with usual seal materials	Usual heat and oil resistant seal materials can be used Lower possibility of contaminant ingression and oil leaks
Simple disposal	Low cost

Manufactured and distributed by MOL-LUB Ltd.
E-mail: lubricants@mol.hu Web: www.mol.hu/en
Technical service: H-1117 Budapest, Neumann János u. 1/E.
Tel: + 36 (1) 464-02-36 E-mail: lubtechdesk@mol.hu

MOL Thermol 46

heat transfer oil

Temperature °C	Kinematic viscosity, mm2/s	Density g/cm3	Specific heat capacity kJ/kgK	Thermal conductivity W/mK	Vapour pressure mbar	Prandtl number
0	546,7	0,889	1,81	0,134		6567
20	126,63	0,876	1,88	0,132		1577
40	43,60	0,863	1,95	0,131		562
50	28,45	0,857	1,99	0,130		373
100	6,50	0,824	2,17	0,126	0,008	92
150	2,74	0,790	2,35	0,123	0,2	41
200	1,56	0,756	2,53	0,119	2,0	25
250	1,03	0,720	2,71	0,116	14,4	17,5
300	0,75	0,684	2,90	0,112	73	13,2
310	0,71	0,677	2,93	0,111	98	12,6
330	0,63	0,662	3,00	0,110	171	11,5

Specifications and approvals

Viscosity grade: ISO VG 46
ISO-L-QB
ISO-L-QC
DIN 51522 Q

Properties

Properties	Typical values
Colour	0,5
Density at 15°C [g/cm3]	0,876
Kinematic viscosity at 40°C [mm2/s]	43,6
Viscosity index	98
Pour point [°C]	-15
Pourpoint [°C]	-15
Flash point (Cleveland) [°C]	232
Conradson carbon residue [mass %]	0,02

The characteristics in table are typical values of the product and do not constitute a specification.

Storage and handling instructions

Store in the original container in dry, properly ventilated area. Keep away from direct flame and other sources of ignition. Protect from direct sunlight.
During transport, storage and use of the product follow the work safety instructions and environmental regulations relating to mineral oil products.
For further details please read the Material Safety Data Sheet of the product.
In the original container under the recommended storage conditions: 48 months
Recommended storage temperature: max. 40°C

Manufactured and distributed by MOL-LUB Ltd.
E-mail: lubricants@mol.hu Web: www.mol.hu/en
Technical service: H-1117 Budapest, Neumann János u. 1/E.
Tel: + 36 (1) 464-02-36 E-mail: lubtechdesk@mol.hu

MOL Thermol 46
heat transfer oil

Ordering information

Custom Tariff Number 27101999

SAP code and packaging:

13301933	MOL Thermol 46 180KG	216.5 l steel drum
13301437	MOL Thermol 46 860KG R1W	IBC (for order only)

Order booking:

Please contact your local distributor or sales partner for ordering details.

Manufactured and distributed by MOL-LUB Ltd.
E-mail: lubricants@mol.hu Web: www.mol.hu/en
Technical service: H-1117 Budapest, Neumann János u. 1/E.
Tel: + 36 (1) 464-02-36 E-mail: lubtechdesk@mol.hu

A.2 Convergence behaviour

A.2.1 Hydraulic Reservoir

As given in the plots below, the convergence behaviour of the hydraulic reservoir with different mesh resolutions is displayed.

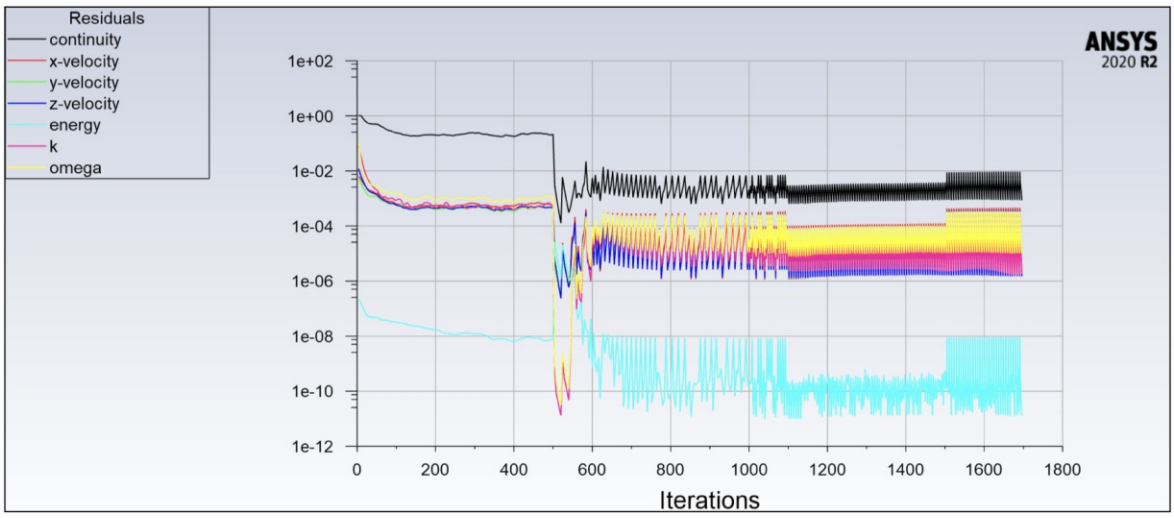

Figure A.1 – Convergence behaviour of the residuals - coarse mesh

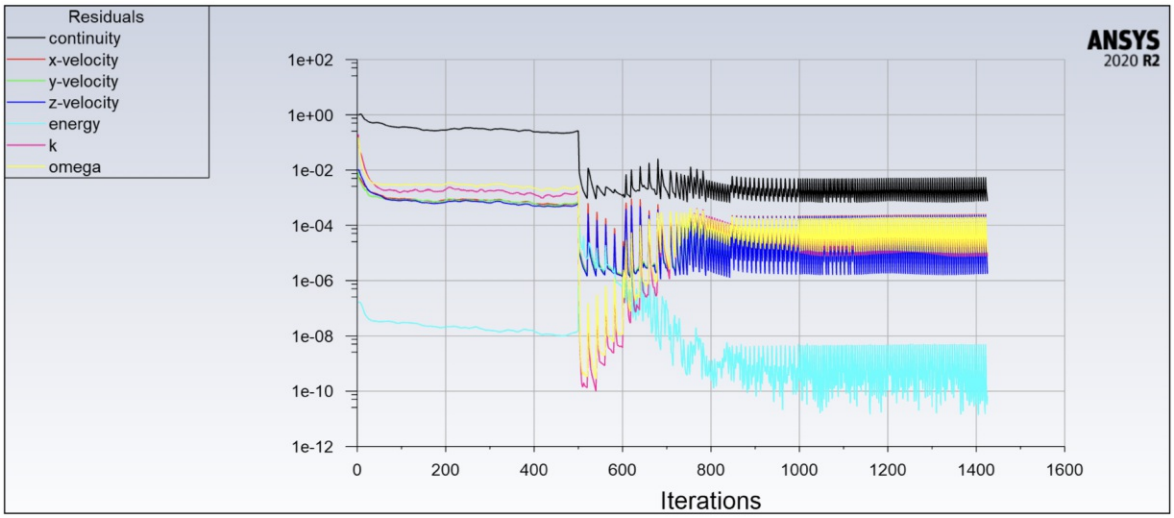

Figure A.2 – Convergence behaviour of the residuals - standard mesh

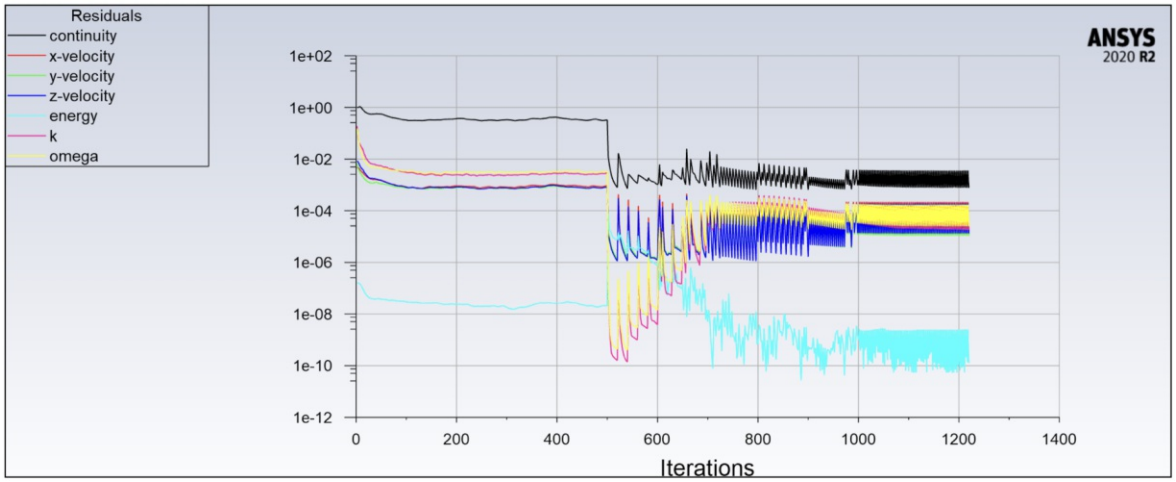

Figure A.3 – Convergence behaviour of the residuals - fine mesh

A.2.2 Straight Pipe & Diffuser Designs

Below the charts of the residuals convergence behaviour of the straight inlet pipe and the four diffuser layouts are given.

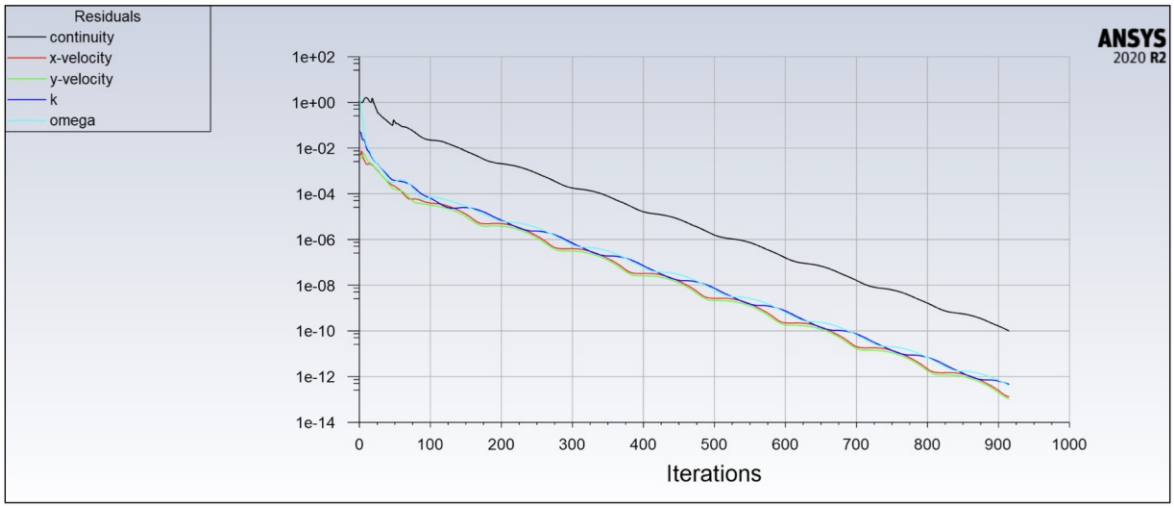

Figure A.4 – Convergence behaviour of the residuals - straight pipe

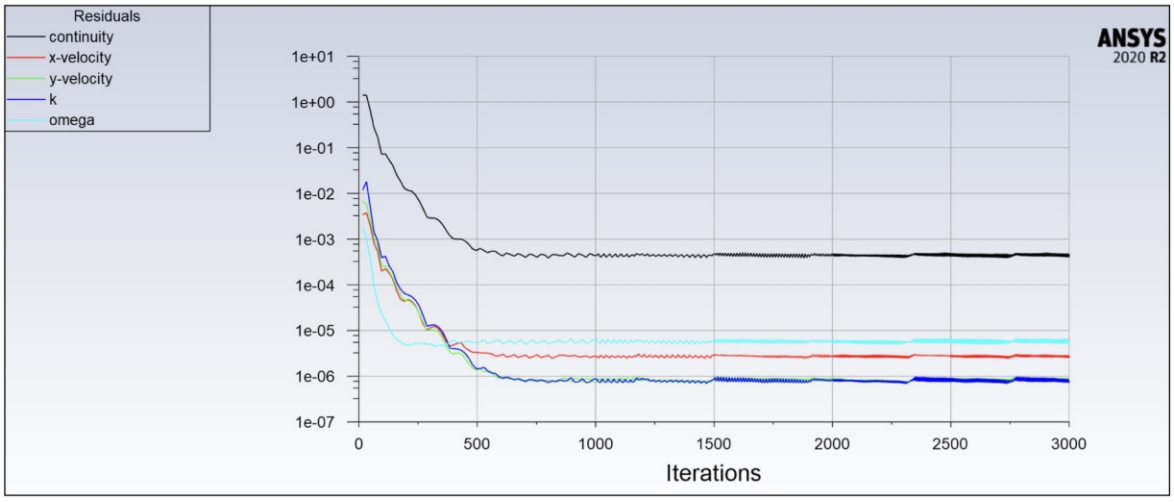

Figure A.5 – Convergence behaviour of the residuals - Design I

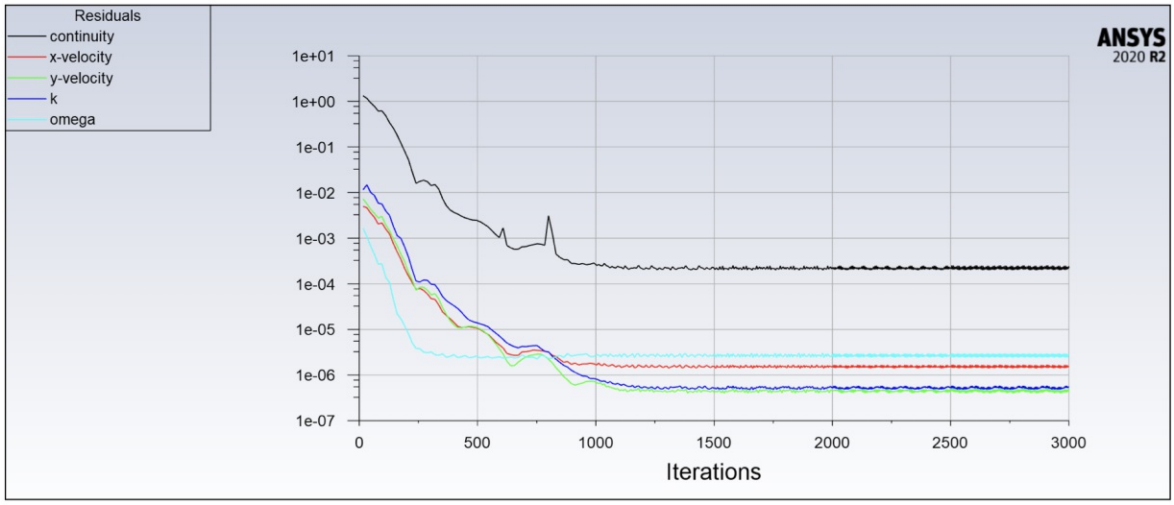

Figure A.6 – Convergence behaviour of the residuals - Design II

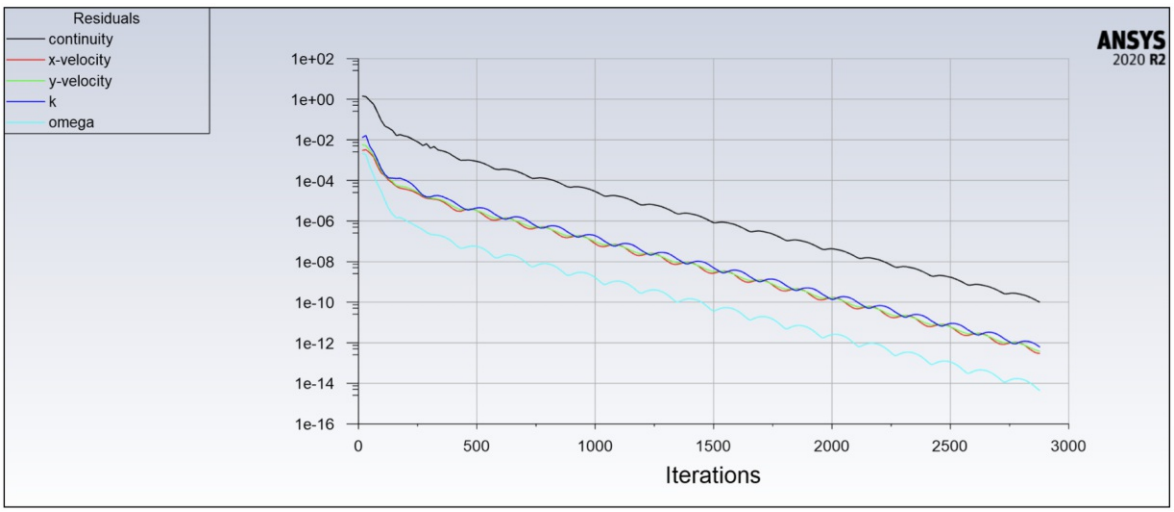

Figure A.7 – Convergence behaviour of the residuals - Design III

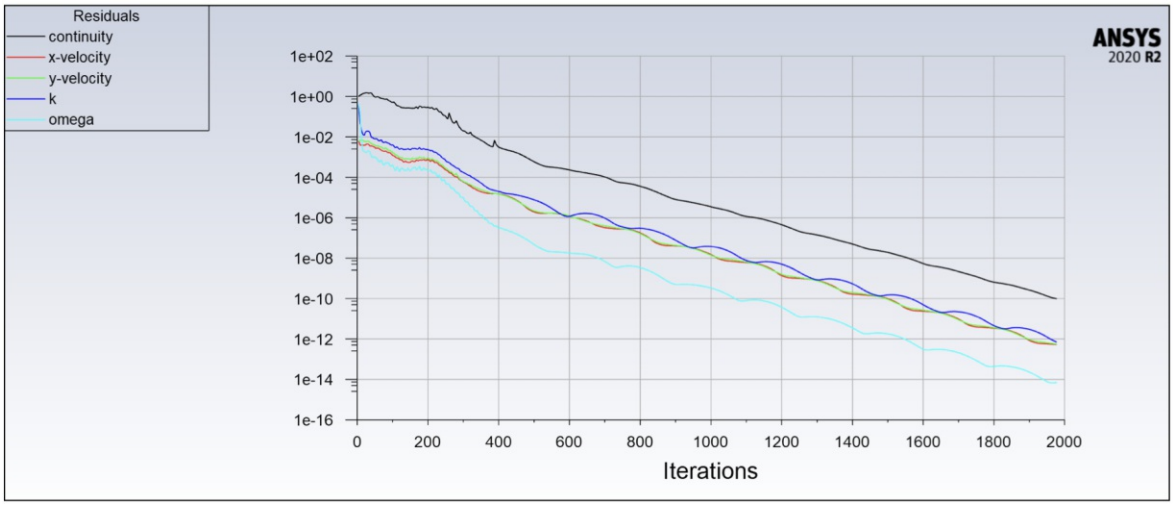

Figure A.8 – Convergence behaviour of the residuals - Design IV